High Altitude Observatory
National Center for Atmospheric Research, Boulder, CO

TIEGCM V1.8 Model Description

May 6, 2005 *Author: Astrid Maute*

e-mail: maute@ucar.edu

Contents

Notation

Variables

$\mathbf{B}$	geomagnetic field
$\mathbf{B}_0$	Earth main magnetic field
B_x, B_y, B_z	geomagnetic main field components (north, east, downward)
$\mathbf{b}_0$	unit vector along $\mathbf{B}_0$
B_{e3}	geomagnetic field strength in $\mathbf{e}_3$ direction [nT]
c	coefficient of the finite difference stencil
$\mathbf{E}$	electric field
E_{d1}, E_{d2}	electric field component in $\mathbf{d}_1$, $\mathbf{d}_2$ direction
H	scale height
h	height
h_0	reference height
h_A	apex height
I_m	inclination angle of dipolar geomagnetic field line at h_0 on a spherical Earth
$\mathbf{J}$	current density
$\mathbf{J}_{\|\|}$	field aligned current density
$\mathbf{J}_M$	magnetospheric current density
$\mathbf{J}$	current density
J_{mr}	radial component of current density
J_{Mr}	radial component of current density for both hemispheres added together
$\mathbf{K}^M$	magnetospheric height integrated current density
$K^M_{m\phi}$	magnetospheric eastward height-integrated current density
$K^M_{m\lambda}$	magnetospheric down–/equatorward height-integrated current density
$K_{m\phi}$	eastward height-integrated current density
$K_{m\lambda}$	down–/equatorward height-integrated current density
$K^D_{m\phi}$	wind driven eastward height-integrated current density
$K^D_{m\lambda}$	wind driven down–/equatorward height-integrated current density
$\overline{m}$	mean molecular mass
m_i	atomic weight of specie i
N_i	density of specie i
n_i	number density of specie i
N_e	electron density
p	atmospheric pressure
p_p	plasma pressure
$ln(p_0/p)$	log pressure levels
R	radius from Earth center to height h
R_0	radius from Earth center to height h_0
T_e	electron temperature
T_i	ion temperature
T_n	neutral temperature
u_n, v_n, w_n	neutral zonal, meridional and vertical wind
W	dimensionless vertical wind
z	geopotential height

Φ	electric potential
Φ_R	reference electric potential
ρ_{ion}	ion density
$\Sigma_{\phi\phi}$	magnetic eastward conductance
$\Sigma_{\lambda\lambda}$	magnetic equator-/downward conductance
$\Sigma_{\phi\lambda}, \Sigma_{\lambda\phi}$	mixed term conductances
$\Sigma^M_{\phi\phi}, \Sigma^M_H$	equivalent magnetospheric conductances
σ_P, σ_H	Pedersen and Hall conductivities
∇	gradient
σ_P, σ_H	Pedersen and Hall conductivities
$\mathbf{u}$	neutral wind
Φ	electric potential
$\mathbf{d}_1, \mathbf{d}_2, \mathbf{d}_3$	magnetic eastward, magnetic down–/equatorward vectors, along the field line
$\mathbf{e}_1, \mathbf{e}_2, \mathbf{e}_3$	magnetic eastward, magnetic down–/equatorward vectors, along the field line
$D = \lvert\mathbf{d}_1 \times \mathbf{d}_2\rvert$	quantity of Earth geomagnetic coordinate system
F	quantity of dipole field
i	longitudinal index
j	latitudinal index
k	height index
$(\cdot)_i, (\cdot)_j, (\cdot)_k$	quantity at $\phi(i)$, $\lambda(j)$, $h(k)$,
$nlon$	number of discrete geographic longitude grid points
$nmlon$	number of discrete geomagnetic longitude grid points
$nlat$	number of discrete geographic latitude grid points
$nmlat$	number of discrete geomagnetic latitude grid points
s_L, s_U	lower and upper boundary for field line integration
wgt	weight for linear interpolation
ϕ, λ	longitude, latitude
ϕ_g, λ_g	geographic longitude, latitude
λ_A	apex latitude
λ_m	modified apex latitude
λ_m^*	irregular modified apex latitude grid distribution
λ_0	equally spaced latitudinal grid distribution in λ_m^*
λ_m^{crb}	modified apex latitude of convection reversal boundary
ϕ_m	modified apex longitude
$(\cdot)_0$	refers to reference height
$(\cdot)(0)$	refers to equally spaced latitudinal grid λ_0
$(\cdot)_A$	quantity at apex of field-line
$(\cdot)_g$	refers to geographic direction
$(\cdot)'$	half pressure level $(\cdot) + \frac{1}{2}$
$(\cdot)_{d1}, (\cdot)_{d2}, (\cdot)_{d3}$	magnetic eastward, down–/equatorward, field-line direction of quantity $(\cdot)$
$(\cdot)_{e1}, (\cdot)_{e2}, (\cdot)_{e3}$	magnetic eastward, down–/equatorward, field-line direction of quantity $(\cdot)$
$(\cdot)_{eq}$	value at the geomagnetic equator
$(\cdot)_{fl}$	value on the geomagnetic field line

$(\cdot)_{m\phi}, (\cdot)_{m\lambda}$	modified apex eastward and down–/equatorward direction of quantity $(\cdot)$
$(\cdot)_{pole}$	values at the geomagnetic poles
$(\cdot)^D$	dynamo part
$(\cdot)^{p,g}$	refers to plasma pressure and gravity contribution
$(\cdot)^T$	both hemispheres added together
$\frac{d(\cdot)}{dt}$	total time rate of change
$\frac{\partial(\cdot)}{\partial}$	partial derivative
lhs, rhs	left and right hand side of electrodynamo equation

Constants

$\mathbf{g}(h_0)$	$870\frac{cm}{s^2}$ $(TIEGCM)$	gravitational acceleration at height h_0
	$945\frac{cm}{s^2}$ $(TIMEGCM)$	gravitational acceleration at height h_0
M_i	$1.6605 \cdot 10^{-24}$ g	mass of unit atomic weight
h_0	$90km(T * GCM)$	height of lower boundary for electrodynamo
h_R	$90km$	reference height
R_E	$6.37122 \cdot 10^8$ cm	mean Earth radius
p_0	$5.0 \cdot 10^{-4}$	standard pressure
k_B	$1.38 \cdot 10^{-16}$ $\frac{cm^2 g}{s^2 K}$	Boltzman constant
R^*	$8.314e7\frac{erg}{moleK}$	gas constant
R_{eq}		Earth radius at the equator

The model code defines these constants to the stated accuracy. We do not mean to imply that these constants are known to this accuracy nor that the low-order digits are significant to the physical approximations employed.

1 Introduction

This report presents the governing equations, physical parameterizations and numerical algorithms used in the NCAR Thermosphere-Ionosphere-Electrodynamics GCM version 1.8. The model description provides help on the major model component, numerics and coding implementation.

The electrodynamic part of TIEGCM is a serial code, which uses finite differencing to discretize the stationary electrostatic equation. We assume that the field–lines are equipotential which reduces the 3D equation to 2D. In addition, at low– and mid–latitude hemispheric symmetry of the electric potential is assumed and therefore the electrodynamo equation is only solved in one hemisphere. At high latitudes the electric potential is prescribed from empirical models e.g. Heelis or Weimer [literature].

Conventions	
command	bold
template filenames	italics
flags	medium bold
directories, files	slanted
`source code`	typewrite
keywords	emphasize

1.1 Brief History

2 Steady–State Electrodynamic Equations

The basic equations of the steady state electrodynamo are shown in this chapter. If an equation is taken from [Rich95]. then the additional equation number refers to the equation number in [Rich95]. In the following the presentation of the equations is based on the coding in the source code and might not look straight forward in many places. For the location in the source code of the equations it is referred to the `subroutine names`.

For longer time scales it is valid to assume steady state electrodynamics with a divergence free current density $\mathbf{J}$. It is also assumed that the conductivity along the magnetic field line is very high, thus there is no electric field component in this direction. Therefore the electrodynamo equation can be reduced to a two dimensional equation.

The current density is divergence free

$$\nabla \cdot \mathbf{J} = 0 \tag{1}$$

The current density has an ohmic component transverse to the magnetic field and parallel to the magnetic field line $\mathbf{J}_{||}$ and a non–ohmic magnetospheric component $\mathbf{J}_M$. In the TIEGCM only the ohmic component transverse to the magnetic field is considered by default. The other two components can be added by the user which is discussed later in chapter 7.3.1 and 7.3.2. The total current density is expressed by (eq. 2.1 in [Rich95])

$$\mathbf{J} = \sigma_P(\mathbf{E} + \mathbf{u} \times \mathbf{B}) + \sigma_H \mathbf{b} \times (\mathbf{E} + \mathbf{u} \times \mathbf{B}) + \mathbf{J}_{||} + \mathbf{J}_M \tag{2}$$

with σ_P and σ_H the Pedersen and Hall conductivities. The neutral wind is denoted by $\mathbf{u}$, the electric field by $\mathbf{E}$ and the geomagnetic field by $\mathbf{B}$ with $\mathbf{b}$ the unit vector parallel to $\mathbf{B}$.

The following relations are used to derive the electrodynamo equation. For details it is referred to [Rich95]. Apex coordinates are used with two sets of base vectors $\mathbf{e}_i$ and $\mathbf{d}_j$ which are calculated in `subroutine apxparm` (see chapter 4). The directions of $\mathbf{e}_1$ and $\mathbf{d}_1$ are more or less in magnetic eastward, $\mathbf{e}_2$ and $\mathbf{d}_2$ in downward or equatorward, and $\mathbf{e}_3$ and $\mathbf{d}_3$ in field line direction. (eq. 3.11-3.13 in [Rich95])

$$\mathbf{e}_1 = \mathbf{d}_2 \times \mathbf{d}_3 \tag{3}$$
$$\mathbf{e}_2 = \mathbf{d}_3 \times \mathbf{d}_1 \tag{4}$$
$$\mathbf{e}_3 = \mathbf{d}_1 \times \mathbf{d}_2 \tag{5}$$

with (eq. 3.8- 3.10 in [Rich95])

$$\mathbf{d}_1 = R_0 cos\lambda_m \nabla \phi_m \tag{6}$$
$$\mathbf{d}_2 = -R_0 sinI_m \nabla \lambda_m \tag{7}$$
$$\mathbf{d}_3 = \frac{\mathbf{b_0}}{|\mathbf{d}_1 \times \mathbf{d}_2|} \tag{8}$$

The geomagnetic longitude and apex latitude are ϕ_m and λ_m, I_m is the inclination of the geomagnetic field, R_0 the radius to the reference height $R_E + h_0$, and b_0 the unit vector in the direction of the geomagnetic field. The neutral wind $\mathbf{u}$ and the electric field $\mathbf{E}$ can be expressed in terms of the base vectors which has the advantage that the components are constant along a magnetic field line (eq. 4.5 in [Rich95]).

$$\mathbf{u} = u_{e1}\mathbf{e}_1 + u_{e2}\mathbf{e}_2 \quad \text{with} \quad u_{ei} = \mathbf{u} \cdot \mathbf{d}_i \tag{9}$$

$$\mathbf{E} = E_{d1}\mathbf{d}_1 + E_{d2}\mathbf{d}_2 \quad \text{with} \quad E_{di} = \mathbf{E} \cdot \mathbf{e}_i \tag{10}$$

The geomagnetic field $\mathbf{B}$ is approximated by the main field $\mathbf{B}_0$. We are using the International Geomagnetic Reference Field (IGRF2000) in TIEGCM and ignore the magnetic perturbation $\Delta\mathbf{B}$ due to the external currents (eq. 3.10, 3.15, 4.4 in [Rich95]).

$$\mathbf{B}_0 = \mathbf{B}_{e3}\mathbf{e}_3 \tag{11}$$

$$\mathbf{b}_0 = \mathbf{d}_3 D \quad \text{with} \quad D = |\mathbf{d}_1 \times \mathbf{d}_2| \tag{12}$$

The current density can be expressed by

$$\mathbf{J} = \sum_{i=1}^{3} J_{ei}\mathbf{e}_i \text{ with } J_{ei} = \mathbf{J} \cdot \mathbf{d}_i \tag{13}$$

Using all the equations from above leads to the current density components J_{e1} and J_{e2} (eq. 5.7, 5.8 in [Rich95])

$$J_{e1} = \sigma_P d_1^2 (E_{d1} + u_{e2}B_{e3}) + (\sigma_H \mathbf{d}_1 \cdot \mathbf{d}_2 - \sigma_H D)(E_{d2} - u_{e1}B_{e3}) \tag{14}$$

$$J_{e2} = (\sigma_P \mathbf{d}_1 \cdot \mathbf{d}_2 + \sigma_H D)(E_{d1} + u_{e2}B_{e3}) + \sigma_P d_2^2 (E_{d2} - u_{e1}B_{e3}) \tag{15}$$

The height integrated current density in magnetic eastward and downward/ equatorward direction are $K_{m\phi}$ and $K_{m\lambda}$. Knowing the current density $\mathbf{J}$ the height integrated components can be calculated by (eq. 5.1, 5.2 in [Rich95])

$$K_{m\phi} = |sinI_m| \int_{s_L}^{s_U} \frac{J_{e1}}{D} ds \tag{16}$$

$$K_{m\lambda} = \mp \int_{s_L}^{s_U} \frac{J_{e2}}{D} ds \tag{17}$$

with the index $(\cdot)_m$ standing for modified apex (see chapter 4). The integration is done along the field line and s_L and s_U are the lower and upper boundary of the ionosphere, i.e. in the TIEGCM v 1.7 model 90 km to the top of the model. The electrostatic field is the gradient of the electric potential. Therefore the component of the electric field are (eq. 5.9, 5.10 in [Rich95])

$$E_{m\phi} = E_{d1} = -\frac{1}{Rcos\lambda_m} \frac{\partial \Phi}{\partial \phi_m} \tag{18}$$

$$E_{m\lambda} = -E_{d2} sinI_m = -\frac{1}{R} \frac{\partial \Phi}{\partial \lambda_m} \tag{19}$$

Inserting equations (18) and (19) into the current density component expressions (14) and (15), which then can be used to calculate the height integrated current density in equations (16) and (17). This leads to (eq. 5.11, 5.12 in [Rich95])

$$K_{m\phi} = \Sigma_{\phi\phi} E_{m\phi} + \Sigma_{\phi\lambda} E_{m\lambda} + K^D_{m\phi} \tag{20}$$

$$K_{m\lambda} = \Sigma_{\lambda\phi} E_{m\phi} + \Sigma_{\lambda\lambda} E_{m\lambda} + K^D_{m\lambda} \tag{21}$$

The terms $K^D_{m\phi}$ and $K^D_{m\lambda}$ are the wind driven height integrated current densities which are the driving forces (eq. 5.19, 5.20 in [Rich95]).

$$K^D_{m\phi} = B_{e3}|sinI_m| \int_{s_L}^{s_U} \left[\frac{\sigma_P d_1^2}{D} u_{e2} + \left(\sigma_H - \frac{\sigma_P \mathbf{d}_1 \cdot \mathbf{d}_2}{D}\right) u_{e1}\right] ds \tag{22}$$

$$K^D_{m\lambda} = \mp B_{e3} \int_{s_L}^{s_U} \left[\left(\sigma_H + \frac{\sigma_P \mathbf{d}_1 \cdot \mathbf{d}_2}{D}\right) u_{e2} - \frac{\sigma_P d_2^2}{D} u_{e1}\right] ds \tag{23}$$

The conductances in the equations (20) and (21) are (eq. 5.13–5.18 in [Rich95])

$$\Sigma_{\phi\phi} = |sinI_m| \int_{s_L}^{s_U} \frac{\sigma_P d_1^2}{D} ds \tag{24}$$

$$\Sigma_{\lambda\lambda} = \frac{1}{|sinI_m|} \int_{s_L}^{s_U} \frac{\sigma_P d_2^2}{D} ds \tag{25}$$

$$\Sigma_H = \int_{s_L}^{s_U} \sigma_H ds \tag{26}$$

$$\Sigma_C = \int_{s_L}^{s_U} \frac{\sigma_P \mathbf{d}_1 \cdot \mathbf{d}_2}{D} ds \tag{27}$$

$$\Sigma_{\phi\lambda} = \pm(\Sigma_H - \Sigma_C) \tag{28}$$

$$\Sigma_{\lambda\phi} = \mp(\Sigma_H + \Sigma_C) \tag{29}$$

$$\tag{30}$$

Since current continuity applies, the divergence of the horizontal current $K_{m\phi}$ and $K_{m\lambda}$ has to be balanced by an upward current density J_{mr} at the top of the ionospheric current sheet layer. (eq. 5.3 in [Rich95])

$$J_{mr} = \frac{-1}{Rcos\lambda_m}\left(\frac{\partial K_{m\phi}}{\partial \phi_m} + \frac{\partial K_{m\lambda} cos\lambda_m}{\partial \lambda_m}\right) \tag{31}$$

Inserting the height integrated current densities (20) and (21) into equation (31) and assuming that in the closed field line region the field lines are equipotential leads to (eq. 5.23 in [Rich95])

$$\begin{aligned} &\frac{\partial}{\partial \phi_m}\left(\frac{\Sigma^T_{\phi\phi}}{cos\lambda_m}\frac{\partial \Phi}{\partial \phi_m} + \Sigma^T_{\phi\lambda}\frac{\partial \Phi}{\partial |\lambda_m|}\right) + \frac{\partial}{\partial |\lambda_m|}\left(\Sigma^T_{\lambda\phi}\frac{\partial \Phi}{\partial \phi_m} + \Sigma^T_{\lambda\lambda} cos\lambda_m \frac{\partial \Phi}{\partial |\lambda_m|}\right) \\ &= R\frac{\partial K^{DT}_{m\phi}}{\partial \phi_m} + R\frac{\partial K^{DT}_{m\lambda cos\lambda_m}}{\partial |\lambda_m|} + R^2 cos\lambda_m J_{Mr} \end{aligned} \tag{32}$$

with $\frac{\partial}{\partial|\lambda_m|} = -\frac{\partial^{SH}}{\partial\lambda_m} = \frac{\partial^{NH}}{\partial\lambda_m}$ and $J_{Mr} = J_{mr}^{SH} + J_{mr}^{NH}$. The values $(\cdot)^T$ denote the sum of the values from northern $(\cdot)^{NH}$ and southern $(\cdot)^{SH}$ hemisphere (eq. 5.24–5.29 [Rich95])

$$\Sigma_{\phi\phi}^T = \Sigma_{\phi\phi}^{NH} + \Sigma_{\phi\phi}^{SH} \tag{33}$$

$$\Sigma_{\lambda\lambda}^T = \Sigma_{\lambda\lambda}^{NH} + \Sigma_{\lambda\lambda}^{SH} \tag{34}$$

$$\Sigma_{\lambda\phi}^T = \Sigma_{\lambda\phi}^{NH} - \Sigma_{\lambda\phi}^{SH} \tag{35}$$

$$\Sigma_{\phi\lambda}^T = \Sigma_{\phi\lambda}^{NH} - \Sigma_{\phi\lambda}^{SH} \tag{36}$$

$$K_{m\phi}^{DT} = K_{m\phi}^{D,NH} + K_{m\phi}^{D,SH} \tag{37}$$

$$K_{m\lambda}^{DT} = K_{m\lambda}^{D,NH} - K_{m\lambda}^{D,SH} \tag{38}$$

In the source code the electrodynamo equation (32) is divided by $\frac{\partial\lambda_m}{cos\lambda_0\partial\lambda_0}$ with λ_0 the equally spaced distribution in modified apex latitudes λ_m which is irregular spaced. The latitudinal distribution is explained in more detail in section 5.

physical field	variable	unit	pressure level	used in
neutral zonal wind:	u_n	$\frac{cm}{s}$	half	dynamo
neutral meridional wind:	v_n	$\frac{cm}{s}$	half	dynamo
dimensionless vertical wind:	W	$\frac{1}{s}$	full	dynamo
geopotential height:	z	cm	full	dynamo
Pedersen conductivity:	σ_P	S	half	dynamo
Hall conductivity:	σ_H	S	half	dynamo
mean molecular mass:	$\overline{m}$	$\frac{g}{mole}$	full	local for w_n
neutral temperature:	T_n	K	half	local for w_n

Table 1: Input fields to `subroutine prep-dynamo`

3 Input to the Electrodynamo

In `subroutine prep-dynamo` fields are prepared for the electrodynamo calculation. The preparation includes reversing the order of the indexing, as well as gathering the fields from the different processors to the master processor. The electrodynamo part is still serial and therefore a gathering of all the subdomains at the beginning and a distribution of the fields to all the subdomains at the end has to be done.

The input to `subroutine prep-dynamo` is summarized in table 1. To calculate the vertical neutral velocity w_n the pressure scale height H $[cm]$ is determined at first, assuming hydrostatic equilibrium for timescales longer than a few minutes.

$$H = \frac{R^* T_n}{\overline{m} g} \tag{39}$$

with R^* the gas constant $[\frac{erg}{moleK}]$, T_n the neutral temperature $[K]$, $\overline{m}$ the mean molecular mass $[\frac{g}{mole}]$ and g acceleration of gravity $[\frac{cm}{s^2}]$. The dimensionless vertical wind W

$$W = -\frac{1}{p}\frac{dp}{dt} \tag{40}$$

is converted to the vertical wind at a constant pressure level by

$$w_n = HW \tag{41}$$

with the pressure p and $\frac{dp}{dt}$ the time rate of change following the fluid motion.

4 Apex Coordinates

The apex and modified apex coordinate system is described in [Rich95]. The apex latitude λ_A is constant along a field line with an apex height h_A.

$$\lambda_A = \pm cos^{-1}(1 + \frac{h_A}{R_{eq}})^{-1/2} \tag{42}$$

with R_{eq} denoting the Earth radius at the equator and the $\pm$ sign for the location of the field line foot point in the northern / southern geomagnetic hemisphere. In the electrodynamo part of TIEGCM modified apex coordinates are used. Modified apex coordinates λ_m have a reference height h_R associated with them.

$$\lambda_m = \pm cos^{-1}(\frac{R_E + h_R}{R_E + h_A})^{-1/2} \tag{43}$$

The mean Earth radius is denoted by R_E assuming a spherical Earth. The reference height h_R is assumed to be the bottom boundary of the ionosphere at $h_R = h_0 = 90km$. One of the advantages for using modified apex latitudes λ_m is that the field line foot point latitudes are continuous at the 90 km (for TIEGCM) lower boundary of the model. Apex latitudes, in contrast, would have a gap at low latitudes since only field line with an apex of at least 90 km could be used for the field line integration. The apex longitude ϕ_A and the modified apex longitude ϕ_m are the same. The apex routines are called once per model run from `program tgcm`. The only input to the calculation of the apex coordinate system in `subroutine apxparm` is the model year. If the electric potential is not calculated in TIEGCM (input flag dynamo==0) the magnetic field information as well as the information needed for the mapping to and from the geographic to the geomagnetic grid is read from an existing NetCDF–file. Note that even if the electric potential is not calculated a potential pattern at high latitude can be prescribed.

In the `subroutine apxparm` the apex coordinates as well as the geomagnetic main field and the base vectors are determined which are summarized in table 2 and later used for the electrodynamo calculation. For each geographic grid point λ_g, ϕ_g the modified apex latitude and longitude λ_m, ϕ_m is calculated. The north–, east– and downward component, respectively, B_x, B_y and B_z, of the main field $\mathbf{B}_0$ and the components of the base vector $\mathbf{d}_1$ and $\mathbf{d}_2$ are determined. The base vectors $\mathbf{d}_1$ and $\mathbf{d}_2$ are more or less in magnetic eastward and down–/equatorward direction. B_{e3} is the main field component in $\mathbf{e}_3$ direction. The vector $\mathbf{e}_3$ is in the direction of the magnetic field line and decreases with increasing altitude. In addition the quantity D is calculated with $D = |\mathbf{d}_1 \times \mathbf{d}_2|$.

The magnetic field quantities $B_z(h_0)$ and $B_0(h_0)$ are in units of [Gauss], $B_{e3}(h_0)$ is in [nT] and the coordinates λ_m and ϕ_m in [rad] with h_0 the reference height (90 km). The mapping from the geographic to the geomagnetic grid and vice versa is done by bilinear interpolation. For each grid point the surrounding grid points of the other grid are determined and the weighting factor for each of these corner grid points are calculated.

variable	description	unit
λ_m, ϕ_m	modified apex coordinates	radian
$B_{e3}(h_0)$	magnetic field component in $\mathbf{e}_3$ direction	nT
$B_z(h_0)$	downward magnetic field component	Gauss
$B_0(h_0)$	main magnetic field strength	Gauss
$\mathbf{d}_1(h_0)$	base vector approx. mag. eastward	-
$\mathbf{d}_2(h_0)$	base vector approx. mag. down–/equatorward	-
$D(h_0)$	$\lvert\mathbf{d}_1 \times \mathbf{d}_2\rvert$	-

Table 2: Apex quantities calculated in `subroutine apxparm` and used for the calculation of the electric potential

5 Latitudinal modified apex grid

Within TIEGCM the distribution of the geomagnetic latitudinal grid points is expressed in two different ways. One is the irregular distribution of modified apex latitudes λ_m^* which gives a better distribution of the latitudinal grid points by having more grid points close to the geomagnetic equator and therefore resolves the equatorial electrojet better. The second expression of latitudinal grid point distribution is equally spaced in modified apex latitude λ_m^* and is denoted by λ_0. The relation between the two is expressed by

$$tan\lambda_m^* = \frac{r_1}{R_0} tan\lambda_0 + \frac{tan\lambda_0{}^{2(\alpha+1))}}{(1 + tan^2\lambda_0)^{\alpha}}^{1/2} \tag{44}$$

with $\alpha = 1.668$ and $r_1 = 1.06e7$. The radius R_0 is the radius to the lower boundary of the model at height h_0. For each equally spaced λ_0 the latitude λ_m^* is calculated. In addition a look up table is set up for equally one degree spaced latitudes λ_m^* with the corresponding λ_0 determined by using Newton's methods. All the arrays are set up in `subroutine consdyn`. Figure 1 shows the distribution of the grid points for λ_0 and λ_m^* for 97 latitudinal grid points.

6 Mapping from and to the geomagnetic grid

The fields in table 3 are mapped from the geographic grid to the geomagnetic grid in `subroutine transf`. `Subroutine transf` is called from `subroutine dynamo` once per timestep. The lower boundary of the TIEGCM model (up to version 1.8) is at 97 km, however the field line integration starts at $h_0 =$ 90 km altitude, where the lower boundary of the ionosphere is assumed to lie. Therefore the fields in table 3 needed for the field line integration have to be extended downward. Three additional height levels (k=-2 to 0) are introduced with k being the height index. The geopotential height z is linearly extrapolated

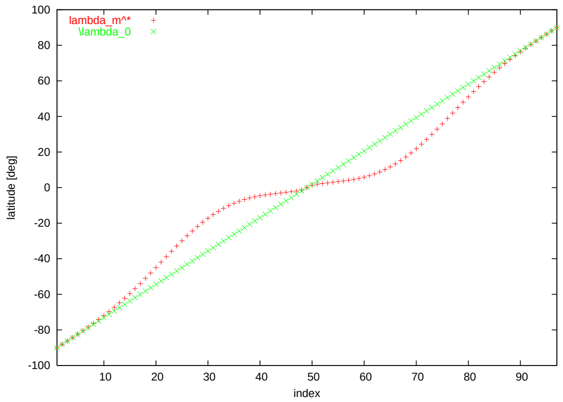

Figure 1: Distribution of modified apex latitude points for λ_0 (crosses) and λ_m^* (pluses)

variable	description	unit	dimension
σ_P	Pedersen conductivity	S	3D
σ_H	Hall conductivity	S	3D
z	geopotential height	cm	3D
$sinI_m(h_0)$	inclination angle	-	2D
$B_{e3}(h_0)$	magnetic field component	T	2D
$\frac{\mathbf{d_1 \cdot d_2}}{D}(h_0)$	base vector quantity	-	2D
$\frac{\mathbf{d_1 \cdot d_1}}{D}(h_0)$	base vector quantity	-	2D
$\frac{\mathbf{d_2 \cdot d_2}}{D}(h_0)$	base vector quantity	-	2D
u_{e1}, u_{e2}	neutral wind components	$\frac{m}{s}$	3D

Table 3: Mapped fields in `subroutine transf`

and the conductivities are assumed to vary exponentially.

$$z(k) = h_0 + (k+2)\left(\frac{z(k=1)-h_0}{3}\right) \quad \text{for k=0 to -2 by -1} \tag{45}$$

$$\sigma_P(k') = \sigma_P(k'=1)exp\left(\frac{z(k+\frac{1}{2}) - z(k=1\frac{1}{2})}{fac_{ped}}\right) \quad \text{for k' =0 to -2 by -1} \tag{46}$$

$$\sigma_H(k') = \sigma_H(k'=1)exp\left(\frac{z(k+\frac{1}{2}) - z(k=1\frac{1}{2})}{fac_{hall}}\right) \quad \text{for k' =0 to -2 by -1} \tag{47}$$

Note that the geopotential height is saved on full pressure levels (k) and the conductivities on half pressure levels ($k' = k+\frac{1}{2}$). Therefore the geopotential height z for the conductivity extension (eq. 46 and 47) is calculated at half pressure levels denoted by e.g. $k' = k + \frac{1}{2}$. The factors at which the conductivities are assumed to decay below the lower boundary of the model are $fac_{ped} = 5. \times 10^5$ and $fac_{hall} = 3. \times 10^5$

The neutral winds $\mathbf{u}$ are assumed to be constant between h_0=90 to 97 km and can be expressed by

$$\mathbf{u} = \mathbf{e}_1 u_{e1} + \mathbf{e}_2 u_{e2} \tag{48}$$

with the base vectors $\mathbf{e}_i$ (see [Rich95]). The base vectors $\mathbf{d}_i$ and $\mathbf{e}_i$ satisfy $\mathbf{d}_i \mathbf{e}_j = \delta_{ij}$ with δ_{ij} the Kronecker delta. The components u_{e1} in magnetic eastward and u_{e2} in down–/equatorward direction at altitude h are calculated by

$$u_{e1}(h) = \mathbf{d}_1(h) \cdot \mathbf{u}(h) \tag{49}$$

$$u_{e2}(h) = \mathbf{d}_2(h) \cdot \mathbf{u}(h) \tag{50}$$

The height variation of $\mathbf{d}_1(h)$ and $\mathbf{d}_1(h)$ is determined by

$$\mathbf{d}_1(h) = [\frac{R_E + h_0}{R_E + h)}]^{3/2} \mathbf{d}_1(h_0) \tag{51}$$

$$\mathbf{d}_2(h) = [\frac{R_E + h_0}{R_E + h)}]^{3/2} \sqrt{\frac{4. - 3.cos^2 \lambda_m(h_0)}{(4. - 3.\frac{R_E+h_0}{R_E+h} cos^2 \lambda_m(h_0)}} \mathbf{d}_2(h_0) \tag{52}$$

with $\lambda_m(h_0)$ the modified apex value at height h_0 which is kept constant vertically and thus representing the quasi–dipole latitude. In addition the following quantities are calculated

$$\frac{\mathbf{d}_1 \cdot \mathbf{d}_1}{D} \tag{53}$$

$$\frac{\mathbf{d}_2 \cdot \mathbf{d}_2}{D} \tag{54}$$

$$\frac{\mathbf{d}_1 \cdot \mathbf{d}_2}{D} \tag{55}$$

These values are calculated at height h_0. The values at the pole need special treatment since we have different longitudinal grid points for one spatial point. Therefore the pole values are extrapolated from the longitudinal averaged values next to the pole.

$$x(l_{pole}) = \frac{9 \sum_{lon} x(l_{pole} \pm 1) - \sum_{lon} x(l_{pole} \pm 2)}{8 \, nlon} \tag{56}$$

with the latitudinal index of the pole l_{pole} and $x(l_{pole} \pm 1)$ denoting the values one grid point off the south– and northpole respectively. The number of geographic longitudinal grid points is $nlon$ and $\sum_{lon}$ denotes the sum over all longitudinal grid points. The following fields are processed: $z(h)$, $\sigma_P(h)$, $\sigma_H(h)$, $u_{e1}(h)$, $u_{e2}(h)$, $\frac{\mathbf{d}_1 \cdot \mathbf{d}_1}{D}$, $\frac{\mathbf{d}_2 \cdot \mathbf{d}_2}{D}$, $\frac{\mathbf{d}_1 \cdot \mathbf{d}_2}{D}$, $sinI_m$, B_{e3}. In addition, periodic points for these fields are added.

The mapping from the geographic to the geomagnetic grid is done for each latitude separately right before the integration along the field line which foot point at this latitude. The field line integration is described in section 8. The geomagnetic equatorial values $\sigma_{P,eq}(h)$, $\sigma_{H,eq}(h)$, $u_{e1,eq}(h)$, $u_{e2,eq}(h)$ have to be known at each geomagnetic latitude and therefore are calculated before the field line integration is done. The mapping from the geographic to the geomagnetic grid is done by a bilinear interpolation. The surrounding geographic grid points for each geomagnetic grid point and the weighting factors for each of the geographic points are determined in `subroutine apxparm`.

7 High Latitude Input

7.1 Weimer

To use the high latitude potential as defined by Weimer the flag POTENTIAL_MODEL = WEIMER in the input file of a TIEGCM has to be set. However the Weimer high latitude potential is not working in the version 1.7 and 1.8 of TIEGCM. Please check newer version carefully.

7.2 Heelis

At high latitude the electric potential pattern can be prescribed as determined by Heelis. The calculation of the electric potential due to Heelis is not described since we didn't work on this part of the code. The Heelis potential pattern is the default if the flag POTENTIAL_MODEL is not specified. The Heelis model is also the basis for the high latitude modifications described in the following sections. Therefore when using these modifications the flag POTENTIAL_MODEL = HEELIS should be set in the input file.

7.3 Modification of the high latitude input

In the electrodynamo equation (32) we neglected so far the current part J_{Mr} between the ionosphere and magnetosphere. The current from the magnetosphere can be influenced by the electric field distribution, however the mechanism is not fully understood. The total field-aligned current between ionosphere and magnetosphere can be described as the divergence of a magnetospheric current $\mathbf{K}^M$

$$J_{Mr} = \frac{1}{R_0 cos\lambda_m}\left(\frac{\partial K_\phi^M}{\partial \phi_m} + \frac{\partial K_{|\lambda|}^M cos\lambda_m}{\partial|\lambda_m|}\right) \tag{57}$$

The height integrated current density $\mathbf{K}^M$ doesn't have to be realistic, but the divergence, i.e. the current J_{Mr}, should be. Using the divergence assures that the integrated field-aligned current over both hemispheres vanishes, and therefore there is no net current into the ionosphere. The two components of the field-aligned current K_ϕ^M and $K_{|\lambda|}^M$, eastward and poleward/ upward, can be differently defined depending on the acting region and the mimicking mechanism. The different contributions are described in the following three subsections. Note that in the default code non of these options is used. To use them one or all of the flags mod_heelis, J_rR and eqMgCnd have to be set to `.true.` in the `dynamo_module`.

7.3.1 Field–aligned current

This part has not been tested yet, however the source code can be found in `subroutine calrhs_jrr`. To use the field–aligned part the flag `J_rR = .true.` in `dynamo_module` has to be set. The magnetospheric current components K_ϕ^M and $K_{|\lambda|}^M$ for the field–aligned current can be derived from a reference potential

Φ_R which we assume is the Heelis potential for now. Using the Heelis potential leads to realistic magnitudes and directions in the current, but might not represent correctly the field-aligned current in the region 1.

$$K_\phi^M = \frac{f_\lambda}{R_0}\left(\frac{\Sigma^T_{\phi\phi}}{cos\lambda_m}\frac{\partial\Phi_R}{\partial\phi_m} + \Sigma^T_{\phi\lambda}\frac{\partial\Phi_R}{\partial|\lambda_m|}\right) \tag{58}$$

$$K_{|\lambda|}^M = \frac{f_\lambda}{R_0 cos\lambda_m}\left(\Sigma^T_{\lambda\phi}\frac{\partial\Phi_R}{\partial\phi_m} + \Sigma^T_{\lambda\lambda}cos\lambda_m\frac{\partial\Phi_R}{\partial|\lambda_m|}\right) \tag{59}$$

The factor f_λ is set such that it's 1 poleward of the the convection reversal boundary λ_m^{crb} and zero equatorward. Thus, the current represents region 1 current and is zero in the region 2.

$$f_\lambda = 1 \quad \text{for} \quad |\lambda_m| \geq \lambda_m^{crb} \tag{60}$$

$$f_\lambda = 0 \quad \text{for} \quad |\lambda_m| < \lambda_m^{crb} \tag{61}$$

In TIEGCM the value for the convection reversal boundary λ_m^{crb} is set to 75^o in the `module cons`. Note that this is not a physical meaningful value since the convection reversal boundary is fixed. For the modified reference potential in section 7.3.3 a variable value for the convection reversal boundary will be used which is set in the `aurora module`. The current components in equations (58) and (59) are calculated in a similar way as the left hand side of the electrodynamo equation, which is described in section 10. The conductance expressions in equation (153)–(156) are used to calculate the current components in equations (58) and (59), and therefore these conductances are input to the `subroutine calrhs_jrr` where the current components eq. (153)–(156) are calculated. The finite difference stencil for the partial derivatives in equations (58) and (59) is set up in `subroutine nsstencil`. In comparison to the set up of the finite difference stencil in section 10 for the left hand side of the electrodynamo equation, here, it's done for both hemispheres and without upwinding technique. Once the finite difference stencil is calculated the electric potential Φ_R is inserted, which is done in `subroutine insert_pot`, to calculate the current components. Although the calculation is done for both hemisphere, it is not necessary since the used Heelis potential is symmetric about the equator and the coefficients of the conductances in equations (153)–(156) are already the sum of the two hemispheres. After calculating the current it is added to the right hand side of the electrodynamo equation (32).

7.3.2 Equivalent magnetospheric conductances

The magnetospheric field-aligned current can be influenced by the electric field distribution in the ionosphere, and therefore depend on the electric potential. The region 2 current with the shielding effect of strong electric fields from high to low latitude is an example of this magnetosphere–ionosphere interaction. The region 2 current can be approximated by a Hall conductor. In addition, the magnetospheric ion loss can be simulated by adding a zonal Pedersen conductance. In TIEGCM we adopt the concept from [Peym93] by using equivalent

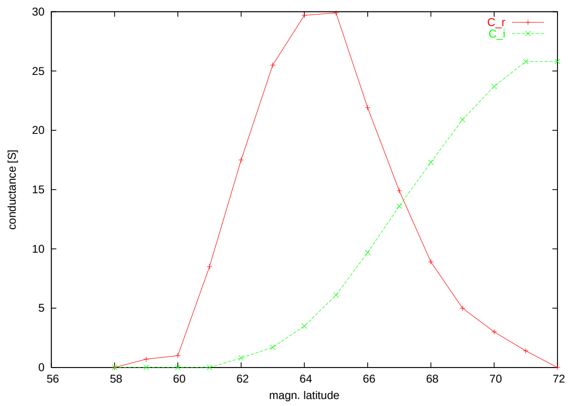

Figure 2: Latitudinal variation of equivalent magnetospheric conductances $\Sigma^M_{\phi\phi}$ (C_r) and Σ^M_H (C_i) for the convection reversal boundary at 72^o.

magnetospheric conductances $\Sigma^M_{\phi\phi}$ and Σ^M_H. The magnetospheric current in eq. (57) can be replaced by

$$K^M_\phi = \frac{-1}{R_0}\left(\frac{\Sigma^M_{\phi\phi}}{cos\lambda_m}\frac{\partial\Phi}{\partial\phi_m} + \Sigma^M_H\frac{\partial\Phi}{\partial|\lambda_m|}\right) \tag{62}$$

$$K^M_{|\lambda|} = \frac{\Sigma^M_H}{R_0 cos\lambda_m}\frac{\partial\Phi_R}{\partial\phi_m} \tag{63}$$

with $\Sigma^M_{\phi\phi}$ and Σ^M_H being the equivalent magnetospheric zonal Pedersen and Hall conductances. The values of $\Sigma^M_{\phi\phi}$ and Σ^M_H are taken from figure 4 in [Peym93] and plotted in figure 2. In `subroutine set_cicr` the equivalent magnetospheric conductances are set up and added to the conductances due to solar ionization and particle precipitation in `subroutine add_cicr`. In figure 2 the equivalent magnetospheric conductances start at 72^o magnetic latitude which is the convection reversal boundary for this specific case. However, the convection reversal boundary varies with the geomagnetic conditions and the location is determined in the `aurora module`. The contributions to the electrodynamo equation due to the equivalent magnetospheric conductances are calculated in a similar way as described in section 8 for the left hand side of the electrodynamo equation. The conductances are calculated on the irregular spaced grid λ^*_m, but for the finite differencing the regular grid λ_0 in λ^*_m is used. Therefore, the difference in the partial derivatives due to the change from λ^*_m to λ_0 have to be taken into account, as described in table 5. The conductance quantities are then prepared for the finite differencing as shown in eq. (153) and (155) and added to the conductances due to solar ionization and particle precipitation. To use the equivalent magnetospheric conductances, the flag eqMgCnd has to be set to `.true.` in the `dynamo_module`.

7.3.3 Modified reference potential

In the region 1 the magnetospheric current in eq.(57) can be represented by the combination of a field–aligned current described in section 7.3.1 and a reference electric potential distribution Φ^R. The later is described in the following. The contribution to the magnetospheric current from a reference potential can be specified by

$$K_\phi^M = \frac{\Sigma^R}{R_0 cos\lambda_m}\frac{\partial(\Phi^R - \Phi)}{\partial\phi_m} \tag{64}$$

$$K_{|\lambda|}^M = \frac{\Sigma^R}{R_0}\frac{\partial(\Phi^R - \Phi)}{\partial\phi_m} \tag{65}$$

The reference conductance Σ^R is not a physical conductance, but determines how strongly the calculated electric potential Φ reflects the reference potential Φ^R. The reference conductance is set to

$$\Sigma^R = \min\left(\Sigma^R_{max}, \Sigma_b[e^{|\lambda_m - \lambda_{crb}|\frac{2}{\alpha_t}} - 1]\right) \quad \text{for} \quad |\lambda_m| \geq \lambda_m^{crb} \tag{66}$$

$$\Sigma^R = 0 \quad \text{for} \quad |\lambda_m| < \lambda_m^{crb} \tag{67}$$

with α_t being the width of the transition zone, here 3^o, equatorward of the convection reversal boundary λ_m^{crb}. The maximum reference conductance Σ^R_{max} is set to $10,000\ S$ and the base conductance Σ_b is 5 S. In the polar cap region the electric potential should be the reference potential. In the source code the Heelis potential is used for the reference potential Φ^R. The convection reversal boundary is denoted by λ_m^{crb}, which varies with the geomagnetic conditions, and is set in the `aurora module`. In figure 3 the latitudinal variation of the reference conductance Σ^R is shown for $\lambda_m^{crb} = 72^o$.

In the source code the calling tree is the following

```
subroutine dynamo
...
if (mod_heelis) then
   if(istep = 1 ) then call set_zigmar
   call add_zigmar
   call diff_rimr
   call add_rimr
endif
...
```

To use the modified reference potential the flag mod_heelis in the `dynamo_module` has to be set to `.true.`. The current in the equations (64) and (65) are calculated like the left hand side of the electrodynamo equation which is described in section 10. The reference conductances Σ^R are calculated according to eq. (66) and (67) in `subroutine set_zigmar`. The coefficients of the reference conductance are added in `subroutine add_zigmar` to the conductances $\Sigma_{\phi\phi}$ and

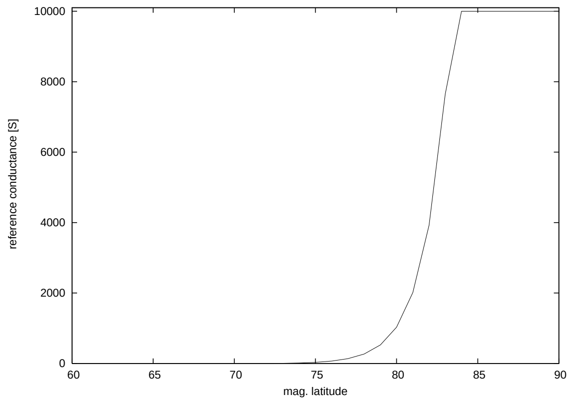

Figure 3: Latitudinal variation of reference conductance Σ^R for $\lambda_m^{crb} = 72^o$

$\Sigma_{\lambda\lambda}$ of the electrodynamo equation. The finite difference stencil is set up in `subroutine diff_rimr` by `subroutine nsstencil`. In comparison to the set up of the stencil for the left hand side of the electrodynamo equation, in section 10, the stencil is calculated for both hemispheres and no upwinding technique are used. Once the finite difference stencil is calculated the electric potential Φ_R is inserted to calculate the additional current for the right hand side of the electrodynamo equation in `subroutine insert_pot`. Although the additional current is determined for both hemisphere separately, this is not necessary since the reference potential and the coefficients of Σ^R are symmetric about the equator.

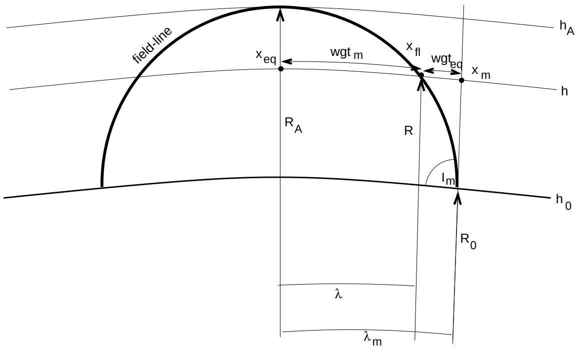

Figure 4: Sketch of geometry for the field–line integration

8 Field line Integration

This section refers to the `subroutine fieldline_integrals` in TIEGCM.

The electrodynamo equation is reduced to two dimensions assuming that the field–lines are equipotential due to the high conductivity along the field–line. The variable along the field line is s, and s_L and s_U are the lower and upper boundary of the line–integration. The inclination of the geomagnetic field–line at the reference height h_0 on an assumed spherical Earth is I_m, and B_{e3} is the component of the geomagnetic field along the field–line. Note that all value,s except the geopotential height z, are stored on half pressure levels to make the integration more convenient.

Approximation of field line values The correct way to do the field line integration would be to trace points along the field line. However, the geomagnetic grid in TIEGCM is not oriented along the field line, and therefore the tracking would involve a two dimensional search and an interpolation to calculate the value on the field line. This can be computational expensive and therefore an approximation, which should be close to the true field line integration, is used. The field line integration is approximated by a height integration combined with an interpolation between the height-varying values at the foot point of the field line (λ_m, h) and the magnetic equator ($\lambda_m = 0, h$) (see. figure 4). Hence, only the height varying values at the foot point location (λ_m, h) are needed. Figure 4 shows schematically a field line with the foot point latitude λ_m at the reference height h_0. The value x_{fl} at height h on the field line is approximated by the value x_{eq} at the equator and height h and the value x_m at foot point latitude λ_m and height h.

$$x_{fl} = wgt_{eq} x_{eq} + wgt_m x_m \tag{68}$$

with the weights wgt_{eq} for the equator value and wgt_m for the foot point value. From figure 4 the weight can be found as

$$wgt_{eq} = \frac{\lambda_m - \lambda}{\lambda_m} \approx \frac{sin(\lambda_m - \lambda)}{\lambda_m} \tag{69}$$

assuming that the difference $\lambda_m - \lambda$ is small, which is true close to the foot point of the field line. Note that determining λ would involve searching for the point on the field line at height h which is time consuming, thus the sinus is used. For field lines which foot point is at mid– and height latitude the value on the field line is essentially the height–varying value at the foot point, since the field line is almost vertical. Close to the magnetic equator the approximation is not so good anymore but the inaccuracy can be neglected when compared to the total field line integration. The term $sin(\lambda_m - \lambda)$ can be substituted by

$$sin(\lambda_m - \lambda) = sin\lambda_m cos\lambda - cos\lambda_m sin\lambda \tag{70}$$

and since for a dipolar field $R = R_A cos^2\lambda$ the $cos\lambda$ and $sin\lambda$ in equation (70) can be substituted by

$$cos\lambda = \sqrt{\frac{R}{R_A}}; \quad sin\lambda = \sqrt{1 - \frac{R}{R_A}}; \tag{71}$$

$$cos\lambda_m = \sqrt{\frac{R_0}{R_A}}; \quad sin\lambda_m = \sqrt{1 - \frac{R_0}{R_A}}; \tag{72}$$

with R_A the radius of the field–line apex (see figure 4). The weighting factors are

$$wgt_{eq} \approx \frac{1}{\lambda_m}\sqrt{1 - \frac{R_0}{R_A}}\sqrt{\frac{R}{R_A}} - \sqrt{\frac{R_0}{R_A}}\sqrt{1 - \frac{R}{R_A}} \tag{73}$$

$$wgt_m = 1 - wgt_{eq} \tag{74}$$

The quantities on the field–line at (h, λ) are therefore approximated by

$$\sigma_P(h,\lambda) = wgt_{eq}(h,\lambda_{eq})\sigma_P(h,\lambda_{eq}) + wgt_m(h,\lambda_m)\sigma_P(h,\lambda_m) \tag{75}$$

$$\sigma_H(h,\lambda) = wgt_{eq}(h,\lambda_{eq})\sigma_H(h,\lambda_{eq}) + wgt_m(h,\lambda_m)\sigma_H(h,\lambda_m) \tag{76}$$

$$u_{e1}(h,\lambda) = wgt_{eq}u_{e1}(h,\lambda_{eq})(h,\lambda_{eq}) + wgt_m(h,\lambda_m)u_{e1}(h,\lambda_m) \tag{77}$$

$$u_{e2}(h,\lambda) = wgt_{eq}u_{e2}(h,\lambda_{eq})(h,\lambda_{eq}) + wgt_m(h,\lambda_m)u_{e2}(h,\lambda_m) \tag{78}$$

Height variation of $\mathbf{d}_1$ and $\mathbf{d}_2$ The apex values $\frac{d_1^2}{D}$, $\frac{d_2^2}{D}$ and $\frac{\mathbf{d}_1 \cdot \mathbf{d}_2}{D}$ are referenced to height h_0 (see section 4). The height variation of these values are small, but should be taken into account. The values $\mathbf{d}_1$, $\mathbf{d}_2$ and D vary with height like

$$\mathbf{d}_1^2(h) = [\frac{R_0}{R}]^3 \mathbf{d}_1^2(h_0) \tag{79}$$

$$\mathbf{d}_2^2(h) = [\frac{R_0}{R}]^3 [\frac{4 - 3cos^2\lambda}{4 - 3\frac{R_0}{R}cos^2\lambda}] \mathbf{d}_2^2(h_0) \tag{80}$$

$$D(h) = \mathbf{d}_1 \cdot \mathbf{d}_2 = (\frac{R_0}{R})^3 (\frac{4 - 3cos^2\lambda}{4 - 3\frac{R_0}{R}cos^2\lambda})^{1/2} D(h_0) \tag{81}$$

Using the dipole approximation $cos^2\lambda = \frac{R}{R_A}$ we can approximate the height variation by

$$\frac{\mathbf{d}_1^2(h)}{D(h)} = (\frac{R_A - \frac{3}{4}R_0}{R_A - \frac{3}{4}R})^{1/2} \frac{\mathbf{d}_1^2(h_0)}{D(h_0)} = \frac{1}{h_{fac}} \frac{\mathbf{d}_1^2(h_0)}{D(h_0)} \tag{82}$$

$$\frac{\mathbf{d}_2^2(h)}{D(h)} = (\frac{R_A - \frac{3}{4}R}{R_A - \frac{3}{4}R_0})^{1/2} \frac{\mathbf{d}_2^2(h_0)}{D(h_0)} = h_{fac} \frac{\mathbf{d}_2^2(h_0)}{D(h_0)} \tag{83}$$

Approximation of ds along the field line Since the integration is done in height rather than along the field–line ds in equations (24)–(29) is expressed in terms of height h.

$$ds = \frac{dh}{|sinI|} \tag{84}$$

However, $sinI$ is going to zero at the magnetic equator and ds would be infinite. Therefore, we have to approximate the relation in equation (84). Starting from the calculation of $sinI$ and using the dipole approximation $cos^2\lambda = \frac{R}{R_A}$ leads to

$$sinI = \frac{2sin\lambda}{\sqrt{4 - 3cos^2\lambda}} = 2\sqrt{\frac{h_A - h}{R_E + 4h_A - 3h}} \tag{85}$$

The numerator $\sqrt{h_A - h}$ varies more than the denominator. Therefore equation (84) is written as

$$ds = \frac{dh}{|sinI|} = -A(h)d\sqrt{h_A - h} = \frac{A(h)dh}{2\sqrt{h_A - h}} \tag{86}$$

with $A(h)$ is the area at height h. The minus sign is introduced since ds should increase with increasing height. From equation (86) follows that the area A(h) and $A(h_0)$ at the reference height is

$$A(h) = \frac{2\sqrt{h_A - h}}{|sinI|}; \quad A(h_0) = \frac{2\sqrt{h_A - h_0}}{|sinI_m|}; \tag{87}$$

Thus, the height varying factor is

$$\frac{A(h)}{A(h_0)} = \frac{2\sqrt{h_A - h}}{|sinI|} \frac{|sinI_m|}{2\sqrt{h_A - h_0}} = \sqrt{\frac{R_A - \frac{3}{4}R}{R_A - \frac{3}{4}R_0}} \tag{88}$$

substituting the inclination angle $sinI$ and $sinI_m$ from equation (85). Inserting equation (87) for $A(h_0)$ in equation (86) will give

$$A(h) = \frac{2\sqrt{h_A - h_0}}{|sinI_m|}\sqrt{\frac{R_A - \frac{3}{4}R}{R_A - \frac{3}{4}R_0}} = A(h_0)h_{fac} \tag{89}$$

The height varying factor $A(h)$ consists of two terms: a height dependent factor h_{fac} which was already defined in equation (83) and a height independent term $A(h_0)$.
The factor $-d\sqrt{h_A - h}$ in equation (84) at the pressure level k can be discretized as follows

$$-d_k\sqrt{h_A - h} = \sqrt{h_A - h_k} - \sqrt{h_A - h_{k+1}} \tag{90}$$

with k being the index of the discrete pressure levels. Note that the geopotential height z is used for h which is stored at full pressure levels. The increment along the field line in eq. (86) can be written as

$$ds = -A(h_0)h_{fac}d\sqrt{h_A - h} \tag{91}$$

Field line integration The following fields are calculated (see also equations 22, 23, 24, 25, 28, 29) using the field line integration

$$\frac{\Sigma_{\phi\phi}}{|sinI_m|} = \int_{s_L}^{s_U} \frac{\sigma_P \mathbf{d}_1^2}{D} ds \tag{92}$$

$$|sinI_m|\Sigma_{\lambda\lambda} = \int_{s_L}^{s_U} \frac{\sigma_P \mathbf{d}_2^2}{D} ds \tag{93}$$

$$\Sigma_C = \int_{s_L}^{s_U} \frac{\sigma_P \mathbf{d}_1 \cdot \mathbf{d}_2}{D} ds \tag{94}$$

$$\Sigma_H = \int_{s_L}^{s_U} \sigma_H ds \tag{95}$$

$$\frac{K_{m\phi}^D}{|sinI_m|} = B_{e3}(h_0)\int_{s_L}^{s_U}\left[\frac{\sigma_P \mathbf{d}_1^2}{D}u_{e2} + \left(\sigma_H - \frac{\sigma_P \mathbf{d}_1 \cdot \mathbf{d}_2}{D}\right)u_{e1}\right]ds \tag{96}$$

$$-K_{m\lambda}^D = \pm B_{e3}(h_0)\int_{s_L}^{s_U}\left[-\frac{\sigma_P \mathbf{d}_2^2}{D}u_{e1} + \left(\sigma_H + \frac{\sigma_P \mathbf{d}_1 \cdot \mathbf{d}_2}{D}\right)u_{e2}\right]ds \tag{97}$$

The field line integration is approximated by taking the sum over all pressure level k (k = -2 to `mlev`, with `mlev` the number of pressure levels). With the approximations of the field line integration in the previous section, the integrals

quantity	name in source code	unit
$\frac{\Sigma_{\phi\phi}}{\lvert sinI_m \rvert}$	zigm11	A/m
$\lvert sinI_m \rvert \Sigma_{\lambda\lambda}$	zigm22	A/m
Σ_C	zigmc	A/m
Σ_H	zigm2	A/m
$\frac{K_{m\phi}^D}{\lvert sinI_m \rvert}$	rim(1)	A/m
$\pm K_{m\lambda}^D$	rim(2)	A/m

Table 4: Field line integrated quantities in `subroutine fieldline_integrals`

in equations (92)–(97) are calculated by

$$\frac{\Sigma_{\phi\phi}}{|sinI_m|} = -A(h_0)\frac{d_1^2}{D}(h_0)\sum_{k=-2}^{mlev}\sigma_{P,k}d_k\sqrt{h_A-h} \tag{98}$$

$$|sinI_m|\Sigma_{\lambda\lambda} = -A(h_0)\frac{d_2^2}{D}(h_0)\sum_{k=-2}^{mlev}\sigma_{P,k}h_{fac,k}^2 d_k\sqrt{h_A-h} \tag{99}$$

$$\Sigma_C = -A(h_0)\frac{\mathbf{d}_1\cdot\mathbf{d}_2}{D}(h_0)\sum_{k=-2}^{mlev}\sigma_{P,k}h_{fac,k}d_k\sqrt{h_A-h} \tag{100}$$

$$\Sigma_H = -A(h_0)\sum_{k=-2}^{mlev}\sigma_{H,k}h_{fac,k}d_k\sqrt{h_A-h} \tag{101}$$

$$\begin{aligned}\frac{K_{m\phi}^D}{|sinI_m|} &= -B_{e3}A(h_0)\sum_{k=-2}^{mlev}\big[\sigma_{P,k}\frac{d_1^2}{D}(h_0)u_{e2,k}+\sigma_{H,k}u_{e1,k}h_{fac,k}- \\ &\quad \sigma_{P,k}\frac{\mathbf{d}_1\cdot\mathbf{d}_2}{D}(h_0)u_{e1,k}h_{fac,k}\big]d_k\sqrt{h_A-h} \\ -K_{m\lambda}^D &= \pm B_{e3}A(h_0)\sum_{k=-2}^{mlev}\big[\sigma_{H,k}u_{e2,k}f_{fac,k}+\sigma_{P,k}\frac{\mathbf{d}_1\cdot\mathbf{d}_2}{D}(h_0)u_{e2,k}h_{fac,k}- \\ &\quad \sigma_{P,k}\frac{d_2^2}{D}(h_0)u_{e1,k}h_{fac,k}^2\big]d_k\sqrt{h_A-h}\end{aligned} \tag{102}$$

After the field line integration is carried out the equatorial field line integral values are set, as well as the equatorial boundary condition is included. Finally, the coefficients of the partial differential equation are modified to take into account that the finite differencing is done with respect to the equally spaced grid with λ_0 which is a function of λ_m^*, although the derivatives are calculated on the irregular grid with λ_m^*. These tasks are carried out in `subroutine transf` of TIEGCM and described in the following.

Equatorial values The values at the geomagnetic equator are approximated since no field line integration can be performed. It is assumed that the average along a field line for a quantities which primarily depend on the Pedersen conductivity σ_P increase by a factor of four from one field line to the next higher one. The average along a field line for quantities mainly dependent on Hall conductivity σ_H vary by 0.83 from one field line to the next higher one. The exact value should not be important for the electric potential calculation, as long as the values are physically reasonable and not too different than those of adjacent field lines. The factor of $\frac{1}{2}$ is introduced to take the adding of the two hemispheres into account, which is done later.

$$\frac{\Sigma_{\phi\phi,eq}}{|sinI_m|} = \frac{1}{2}\frac{1}{4}\frac{\Sigma_{\phi\phi,eq+\Delta\lambda_m}}{|sinI_m|} \tag{103}$$

$$|sinI_m|\Sigma_{\lambda\lambda,eq} = \frac{1}{2}\frac{1}{4}|sinI_m|\Sigma_{\lambda\lambda,eq+\Delta\lambda_m} \tag{104}$$

$$\Sigma_{C,eq} = \frac{1}{2}\frac{1}{4}\Sigma_{C,eq+\Delta\lambda_m} \tag{105}$$

$$\Sigma_{H,eq} = \frac{1}{2}0.12\Sigma_{H,eq+\Delta\lambda_m} \tag{106}$$

$$\frac{K^D_{m\phi,eq}}{|sinI_m|} = \frac{1}{2}0.12\frac{K^D_{m\phi,eq+\Delta\lambda_m}}{|sinI_m|} \tag{107}$$

$$K^D_{m\lambda,eq} = \frac{1}{2}0.12K^D_{m\lambda,eq+\Delta\lambda_m} \tag{108}$$

Equatorial boundary condition At the equator the northward height integrated current density has to vanish (see [Rich95] eq. 5.30 or 5.31).

$$K_{m\lambda} = 0 \tag{109}$$

Solving equation (5.31) in [Rich95] for $\frac{\partial\Phi}{\partial\lambda_m}$ leads to

$$\frac{\partial\Phi}{\partial\lambda_m} = \frac{1}{\Sigma_{\lambda\lambda}}[R_0K^D_{m\lambda} - \frac{\Sigma_{\lambda\phi}}{cos\lambda_m}\frac{\partial\Phi}{\partial\phi_m}] \tag{110}$$

which is substituted into the electrodynamo equation (32). Due to the special geometry at the geomagnetic equator with horizontal field lines we can use the Cowling conductivity

$$\Sigma_{Cowling} = \Sigma_{\phi\phi} - \frac{\Sigma_{\phi\lambda}\Sigma_{\lambda\phi}}{\Sigma_{\lambda\lambda}} \tag{111}$$

and get

$$\begin{aligned}&\frac{\partial}{\partial\phi_m}[\frac{\Sigma_{Cowling}}{cos\lambda_m}\frac{\partial\Phi}{\partial\phi_m}] + \frac{\partial}{\partial|\lambda_m|}[\Sigma_{\lambda\phi}\frac{\partial\Phi}{\partial\phi_m} + \Sigma_{\lambda\lambda}cos\lambda_m\frac{\partial\Phi}{\partial|\lambda_m|}] = \\ &R_0\frac{\partial}{\partial\phi_m}[K^D_{m\phi} - \frac{\Sigma_{\phi\lambda}}{\Sigma_{\lambda\lambda}}K^D_{m\lambda}] + R_0\frac{\partial K^{DT}_{m\lambda cos\lambda_m}}{\partial|\lambda_m|}\end{aligned} \tag{112}$$

Therefore the value $\frac{\Sigma_{\phi\phi}}{|sinI_m|}$ (see table 4) at the geomagnetic equator has to be modified by

$$\frac{\Sigma^{mod}_{\phi\phi}}{|sinI_m|} = \left[\frac{\Sigma_{\phi\phi}}{|sinI_m|} - \frac{\Sigma_{\phi\lambda}\Sigma_{\lambda\phi}}{\Sigma_{\lambda\lambda}|sinI_m|}\right]_{eq} \tag{113}$$

as well as the value $\frac{K^D_{m\phi}}{|sinI_m|}$ (see table 4) by

$$\frac{K^{D,mod}_{m\phi,eq}}{|sinI_m|} = \left[\frac{K^D_{m\phi}}{|sinI_m|} - \frac{\Sigma_{\phi\lambda}K^D_{m\lambda}}{\Sigma_{\lambda\lambda}|sinI_m|}\right]_{eq} \tag{114}$$

Transformation from λ^*_m to λ_0 The geomagnetic latitudinal grid λ^*_m is irregular spaced in latitude. For convenience the derivatives are taken with respect to λ_0 which is equally spaced in λ^*_m. Therefore, the electrodynamo equation (see also eq. 32) can be written with $\lambda_m = \lambda^*_m$

$$\begin{aligned}&\frac{\partial}{\partial\phi_m}\left(\frac{\Sigma_{\phi\phi}}{cos\lambda^*_m}\frac{\partial\Phi}{\partial\phi_m} + \Sigma_{\phi\lambda}\frac{\partial\Phi}{\partial|\lambda^*_m|}\right) + \frac{\partial}{\partial|\lambda^*_m|}\left(\Sigma_{\lambda\phi}\frac{\partial\Phi}{\partial\phi_m} + \Sigma_{\lambda\lambda}cos\lambda^*_m\frac{\partial\Phi}{\partial|\lambda^*_m|}\right)\\ &= R\frac{\partial K^D_{m\phi}}{\partial\phi_m} + R\frac{\partial K^D_{m\lambda}cos\lambda^*_m}{\partial|\lambda^*_m|} + R^2 cos\lambda^*_m J_{mr}\end{aligned} \tag{115}$$

and has to be transformed to account for the change to λ_0. Note that the longitude is not changing. The whole equation is multiplied by $\frac{\partial\lambda^*_m}{\partial\lambda_0}$ which lead to

$$\begin{aligned}&\frac{\partial\lambda^*_m}{\partial\lambda_0}\frac{\partial}{\partial\phi_m}\left(\frac{\Sigma_{\phi\phi}}{cos\lambda_0}\frac{cos\lambda_0}{cos\lambda^*_m}\frac{\partial\Phi}{\partial\phi_m} + \Sigma_{\phi\lambda}\frac{\partial\lambda_0}{\partial\lambda^*_m}\frac{\partial\Phi}{\partial\lambda_0}\right)+\\ &\frac{\partial\lambda^*_m}{\partial\lambda_0}\frac{\partial}{\partial\lambda^*_m}\left(\Sigma_{\lambda\phi}\frac{\partial\Phi}{\partial\phi_m} + \Sigma_{\lambda\lambda}cos\lambda_0\frac{cos\lambda^*_m}{cos\lambda_0}\frac{\partial\lambda_0}{\lambda^*_m}\frac{\partial\Phi}{\partial\lambda_0}\right)\\ &= R_0\frac{\partial\lambda^*_m}{\partial\lambda_0}\frac{\partial K^D_{m\phi}}{\partial\phi_m} + R_0\frac{\partial K^D_{m\lambda}cos\lambda_0\frac{cos\lambda^*_m}{cos\lambda_0}}{\partial\lambda_0} + R_0^2 cos\lambda_m\frac{\partial\lambda^*_m}{\partial\lambda_0}J_{mr}\end{aligned} \tag{116}$$

The electrodynamo equation is multiplied by $\frac{\partial\lambda^*_m}{\partial\lambda_0}$ to avoid problems at the geomagnetic equator due to $\frac{1}{sinI_m}$ which is not defined at the equator, however $\frac{1}{sinI_m}\frac{\partial\lambda_0}{\partial\lambda^*_m}$ is defined at the equator. The quantities after the transformation are listed in table (5) with $(\cdot)(0)$ denoting the quantity $(\cdot)$ referenced to λ_0. The polar values of the conductances are calculated by extrapolated weighting e.g. for a quantity x the polar value is determined by

$$x(j_{pole}) = \frac{1}{3\text{nmlon}}\left[4.\sum_{i=1}^{nmlon} x(i, j_{pole} \mp 1) - \sum_{i=1}^{nmlon} x(i, j_{pole} \mp 2)\right] \tag{117}$$

with $nmlon$ the number of longitudes and j_{pole} the latitudinal index at the north / south pole and the $\mp$ sign referring to the poles respectively. The height integrated current densities $K^D_{m\phi}(0)$ and $K^D_{m\lambda}(0)$ are averaged over the pole. Note that the electrodynamo equation is not solved at the pole, however the polar values are needed for the finite differencing.

quantity	name in source code	unit
$\Sigma_{\phi\phi}(0) = \Sigma_{\phi\phi}\frac{cos\lambda_0}{cos\lambda_m^*}\frac{\partial\lambda_m^*}{\partial\lambda_0}$	zigm11	S
$\Sigma_{\lambda\lambda}(0) = \Sigma_{\lambda\lambda}\frac{cos\lambda_m^*}{cos\lambda_0}\frac{\partial\lambda_0}{\partial\lambda_m^*}$	zigm22	S
$\Sigma_C(0) = \Sigma_C$	zigmc	S
$\Sigma_H(0) = \Sigma_H$	zigm2	S
$K_{m\phi}^D(0) = K_{m\phi}^D\frac{\partial\lambda_m^*}{\partial\lambda_0}$	rim(1)	A/m
$\pm K_{m\lambda}^D(0) = \pm K_{m\lambda}^D\frac{cos\lambda_m^*}{cos\lambda_0}$	rim(2)	A/m

Table 5: Quantities after the transformation at the end of `subroutine transf`

9 Gravity and plasma pressure driven current

9.1 Gravity Driven Current

This section refers to the `subroutine magpres_grav` in TIEGCM. Note that the units in this section are the units used in the source code of TIEGCM. By default the gravity driven current is calculated for a model run. To omit the gravity and plasma pressure driven current the flag j_pg=.false. in `magpres_g_module` has to be set.

The current driven by gravity can be calculated by

$$\mathbf{J}_g(h) = \frac{1}{\mathbf{B}(h)^2} \rho_{ion} \mathbf{g}(h) \times \mathbf{B}(h) \tag{118}$$

with $\mathbf{B}$ [Gauss] the Earth main magnetic field, the ion density ρ_{ion} $[\frac{1}{cm^3}]$, and $\mathbf{g}(h)$ $[\frac{cm}{s^2}]$ the gravitational acceleration at height h. The gravitational field gets weaker with height and therefore the gravitational acceleration at reference height $h_0 = 90\ km$ is scaled by

$$\mathbf{g}(h) = \left(\frac{R_0}{R}\right)^2 \mathbf{g}(h_0) \tag{119}$$

with $R = R_E + h$ and R_E the mean Earth radius. The radius of the reference height is $R_0 = R_E + h_0$. The ion density is determined by

$$\rho_{ion} = M_i \sum_i n_i m_i \quad \text{with} \quad i = O^+, O^{2+}, N^+, N^{2+}, NO^+ \tag{120}$$

with the mass of a unit atomic weight M_i [g], n_i $[\frac{1}{cm^3}]$ the ion number density of the species i and m_i its corresponding atomic weight. Combining equations (119) and (120) and converting from $[\frac{g}{s^2 cm^2}]$ to $[\frac{kg}{s^2 m^2}]$ will introduce an additional factor of 10 (see equation 122).
The height variation of the Earth main magnetic field is approximated by

$$\mathbf{B}(h) = \left(\frac{R_0}{R}\right)^3 \mathbf{B}(h_0) \tag{121}$$

with $\mathbf{B}(h_0)$ [Gaus] referenced to h_0. The components of the main field are $\mathbf{B} = (b_x, b_y, b_z)$ the north–, east– and downward components or $\mathbf{B} = (b_{\phi_g}, b_{\lambda_g}, b_{z_g})$ with ϕ_g, λ_g and z_g the directions in geographic longitude, latitude and upward height respectively. The current in $[\frac{A}{cm^2}]$ due to the gravitational force is calculated at half pressure levels $k + \frac{1}{2}$ by

$$\mathbf{J}_{g,k+\frac{1}{2}} = 10 \frac{R}{R_0} \frac{1}{\mathbf{B}_0^2} \rho_{ion} g(h_0)(b_x, -b_y, 0) \tag{122}$$

Note that in the TIEGCM code most quantities are evaluated at half levels $k + \frac{1}{2}$ and stored at level k' with $(\cdot)'$ denoting the half levels $(\cdot) + \frac{1}{2}$ in contrast to k which is the full pressure level k. Therefore R and ρ_{ion} in equation (122) must be evaluated at the half level $k + \frac{1}{2}$.

9.2 Plasma Pressure Gradient Driven Current

This section refers to the `subroutine magpres_grav` in TIEGCM. Note that the units in this section are the units used in the source code of TIEGCM. The plasma pressure gradient driven current is calculated by default for a model run. To omit the gravity and plasma pressure driven current the flag j_pg=.false. in `magpres_g_module` has to be set.

The current due to the plasma pressure gradient ∇p_p is

$$\mathbf{J}_p = -\frac{1}{\mathbf{B}(h)^2}\nabla p_p \times \mathbf{B}(h) \tag{123}$$

with the plasma pressure

$$\nabla p_p = k_B \nabla[(T_i + T_e)N_e] \tag{124}$$

The Boltzmann constant is denoted by k_B; T_i, T_e and N_e are the ion temperature [K], the electron temperature [K] and the electron density $[\frac{1}{cm^3}]$. The gradient ∇ is taken in the geographic direction $(\nabla_{\phi_g}, \nabla_{\lambda_g}, \nabla_{z_g})$.
The vertical gradient $\nabla_{z_g} p_p$ is approximated at the half pressure level $k + \frac{1}{2}$ by

$$\begin{aligned}\nabla_{z_g} p_{p,k+\frac{1}{2}} = 10 k_B \Bigg[& \frac{N_{e,k+1} - N_{e,k}}{z_{k+1} - z_k}(T_i + T_e)_{k+\frac{1}{2}} + \\ & \frac{(T_i + T_e)_{k+1} - (T_i + T_e)_k}{z_{k+1} - z_k} N_{e,k+\frac{1}{2}} \Bigg]\end{aligned} \tag{125}$$

with the geopotential height z in [cm]. The factor of 10 takes the conversion from $[\frac{g}{s^2 cm^2}]$ to $[\frac{kg}{s^2 m^2}]$ into account.
The plasma pressure gradient in geographic eastward direction at the half pressure level $k + \frac{1}{2}$ and geographic longitude ϕ_g and geographic latitude λ_g is approximated by

$$\begin{aligned}\nabla_{\phi_g} p_{p,k+\frac{1}{2}} = & 10 k_B \frac{1}{2\Delta\phi R_{k+\frac{1}{2}} cos\lambda_g} \Bigg[\\ & \big(N_e(\phi_g + \Delta\phi_g) - N_e(\phi_g - \Delta\phi_g)\big)_{k+\frac{1}{2}} (T_i(\phi_g) + T_e(\phi_g))_{k+\frac{1}{2}} + \\ & \big((T_i + T_e)(\phi_g + \Delta\phi_g) - (T_i + T_e)(\phi_g - \Delta\phi_g)\big)_{k+\frac{1}{2}} N(\phi_g)_{e,k+\frac{1}{2}} \Bigg]\end{aligned} \tag{126}$$

with $\Delta\phi_g$ the discrete step size in the eastward direction and the radius $R_{k+\frac{1}{2}}$ at the half pressure level.
The plasma pressure gradient in geographic north direction at the half pressure level $k + \frac{1}{2}$ and geographic longitude ϕ_g and geographic latitude λ_g is approxi-

mated by

$$\nabla_{\lambda_g} p_{p,k+\frac{1}{2}} = 10 k_B \frac{1}{2\Delta\lambda R_{k+\frac{1}{2}}} \Big[\big(N_e(\lambda_g+\Delta\lambda_g) - N_e(\lambda_g-\Delta\lambda_g)\big)_{k+\frac{1}{2}} (T_i(\lambda_g)+T_e(\lambda_g))_{k+\frac{1}{2}} + \big((T_i+T_e)(\lambda_g+\Delta\lambda_g) - (T_i+T_e)(\lambda_g-\Delta\lambda_g)\big)_{k+\frac{1}{2}} N(\lambda_g)_{e,k+\frac{1}{2}} \Big] \tag{127}$$

with $\Delta\lambda_g$ the discrete step size in the northward direction. At the geographic poles we set

$$\nabla_{\lambda_g} p_{p,k+\frac{1}{2}}(\lambda_g = \pm 90^\circ) = 0 \tag{128}$$

Inserting the derivatives (125), (126) and (127) into equation (124) lead to

$$\nabla p_p = 10 k_B \begin{pmatrix} \nabla_{\phi_g} \\ \nabla_{\lambda_g} \\ \nabla_{z_g} \end{pmatrix} [(T_i+T_e)N_e]_{\phi_g,\lambda_g,k+\frac{1}{2}} \tag{129}$$

with ∇p_p in $[\frac{kg}{s^2 m^2}]$. The cross product with the geomagnetic field vector from equation (123) can be written as

$$\begin{aligned} \mathbf{J}_{p,\phi_g,\lambda_g,k+\frac{1}{2}} &= -\frac{10 k_B}{\mathbf{B}_0^2}\left(\frac{R}{R_0}\right)^3 \begin{pmatrix} \nabla_{\phi_g} \\ \nabla_{\lambda_g} \\ \nabla_{z_g} \end{pmatrix} \times \begin{pmatrix} b_y \\ b_x \\ -b_z \end{pmatrix} [(T_i+T_e)N_e]_{\phi_g,\lambda_g,k+\frac{1}{2}} \\ &= -\frac{10 k_B}{\mathbf{B}_0^2}\left(\frac{R}{R_0}\right)^3 \begin{pmatrix} -\nabla_{\lambda_g} b_z - \nabla_{z_g} b_x \\ \nabla_z b_y + \nabla_{\phi_g} b_z \\ \nabla_{\phi_g} b_x - \nabla_{\lambda_g} b_y \end{pmatrix} [(T_i+T_e)N_e]_{\phi_g,\lambda_g,k+\frac{1}{2}} \end{aligned} \tag{130}$$

The height variation of the magnetic field is approximated by the factor $(\frac{R}{R_0})^3$. The calculated current vectors $\mathbf{J}_g$ and $\mathbf{J}_p$ have to be rotated to point in the geomagnetic direction.

$$\frac{1}{D} J_{e1}^{p,g} = \frac{\mathbf{d}_1}{D} \cdot \mathbf{J}_{pg} \tag{131}$$

$$\frac{1}{D} J_{e2}^{p,g} = \frac{\mathbf{d}_2}{D} \cdot \mathbf{J}_{pg} \tag{132}$$

with $\mathbf{d}_1$ and $\mathbf{d}_2$ denoting the vectors in quasi magnetic eastward and down/equatorward direction. The quantity D varies with the strength of the geomagnetic field and the distortion of the geomagnetic field from a pure dipole field. The quantity D can be calculated by using the vectors $\mathbf{d}_1$ and $\mathbf{d}_2$

$$D = |\mathbf{d}_1 \times \mathbf{d}_2| \tag{133}$$

The vectors $\mathbf{d}_1(h_0)$ and $\mathbf{d}_2(h_0)$ as well as $D(h_0)$ are only calculated at the reference height h_0. The height variation is approximated by

$$\mathbf{d}_1(h) = \mathbf{d}_1(h_0)\left(\frac{R_0}{R}\right)^{\frac{3}{2}}; \qquad \mathbf{d}_2(h) = \mathbf{d}_2(h_0)\left(\frac{R_0}{R}\right)^{\frac{3}{2}} \frac{\sqrt{4-3cos^2\lambda_m}}{\sqrt{4-3\frac{R_0}{R}cos^2\lambda_m}} \quad (134)$$

Considering equation (133) the quantity $\frac{\mathbf{d}_1}{D}$ varies like $\frac{1}{\mathbf{d}_2}$ and $\frac{\mathbf{d}_2}{D}$ varies like $\frac{1}{\mathbf{d}_1}$. The current at top pressure level of the model is extrapolated using

$$J^{p,g}_{e1,k_{max}+\frac{1}{2}} = \frac{3}{2}J^{p,g}_{e1,k_{max}-\frac{1}{2}} - \frac{1}{2}J^{p,g}_{e1,k_{max}-\frac{3}{2}} \quad (135)$$

$$J^{p,g}_{e2,k_{max}+\frac{1}{2}} = \frac{3}{2}J^{p,g}_{e2,k_{max}-\frac{1}{2}} - \frac{1}{2}J^{p,g}_{e2,k_{max}-\frac{3}{2}} \quad (136)$$

with $k_{max} + \frac{1}{2}$ the index of the highest pressure level.

9.3 Field–line Integration

This section describes how the gravity and plasma pressure gradient driven current is added to forcing of the electrodynamo equation. The gravity and plasma pressure gradient driven current is therefore added to the current driven by the neutral wind. The current of the different sources are combined in `subroutine fieldline_integrals`, before the field line integration. The field line integration itself is described in section 8.
The height–integrated eastward current density $K_{m\phi}$, see eq. (22), is calculated and included on the right hand side of the electrodynamo equation (32). The current $J^{p,g}_{e1}$ due to gravity and plasma pressure gradient is added.

$$K_{m\phi} = |sinI_m| \int_{s_L}^{s_U} \frac{J_{e1}}{D} ds = B_{e3}|sinI_m| \int_{s_L}^{s_U} \left[\frac{J^D_{e1}}{D} + \frac{J^{p,g}_{e1}}{B_{e3}D}\right] ds \quad (137)$$

with s the line–integral variable and s_L and s_U the lower and upper boundary of the line–integration. The inclination of the geomagnetic field line at the reference height h_0 on an assumed spherical Earth is I_m and B_{e3} the component of the geomagnetic field along the field–line. The eastward current J_{e1} has a contribution from the neutral winds J^D_{e1} and from the plasma pressure and gravity term $J^{p,g}_{e1}$.
The field–line integration is approximated by a height–integration combined with an interpolation between the height-varying values at the foot point of the field line (λ_m) and at the magnetic equator ($\lambda = 0$) which is described in section 8. Figure 4 shows schematically that for a field line with the foot point at the reference height h_0 and latitude λ_m the value x_{fl} at height h on the field line is approximated by the value x_{eq} at the equator and value x_m at foot point λ_m and height h. The calculation of the weighting factors x_{fl} and wgt_{eq} for the interpolation are described in section 8 equations (68) and (69).

Therefore the eastward current at (λ, h) on the field line is approximated by

$$J^{p,g}_{e1}(\lambda, h) = wgt_{eq}(h, \lambda_{eq})J^{p,g}_{e1,eq}(\lambda_{eq}, h) + wgt_m(\lambda_m, h)J^{p,g}_{e1,m}(\lambda_m, h) \quad (138)$$

Since the integration is done in height rather than along the field–line, ds in equation 137 is expressed in terms of height h. The conversion from field line integration to height is shown in section 8. The increment ds along the field line is substituted by eq. (91). The contribution $K_{m\phi}^{p,g}$ to the height integrated eastward current is the sum over all pressure level k

$$\frac{K_{m\phi}^{p,g}}{|sinI_m|} = B_{e3}(h_0)A(h_0)\sum_k \left[\frac{10^4 J_{e1}^{p,g}(\lambda, h_{k+\frac{1}{2}})}{B_{e3}(h_0)D(h_{k+\frac{1}{2}})}\right] 10^{-2} h_{fac}(-d\sqrt{h_A - h_{k+\frac{1}{2}}}) \tag{139}$$

The factor 10^4 converts the current from $[\frac{A}{cm^2}]$ to $[\frac{A}{m^2}]$ and the factor 10^{-2} converts ds from [cm] to [m]. The north–/upward height integrated current density is

$$K_{m\lambda} = \mp \int_{s_L}^{s_U} \frac{J_{e2}}{D} ds = \mp B_{e3} \int_{s_L}^{s_U} \left[\frac{J_{e2}^D}{D} + \frac{J_{e2}^{p,g}}{B_{e3}D}\right] ds \tag{140}$$

With the above mentioned approximation of the field line integration the contribution from the plasma pressure gradient and the gravity driven current is the sum over all pressure level k

$$K_{m\lambda}^{p,g} = \pm B_{e3}(h_0)A(h_0)\sum_k \left[\frac{10^4 J_{e2}^{p,g}(\lambda, h_{k+\frac{1}{2}}])}{B_{e3}(h_0)D(h_{k+\frac{1}{2}})}\right] 10^{-2} h_{fac}(d\sqrt{h_A - h_{k+\frac{1}{2}}}) \tag{141}$$

10 Finite Differencing

Hemispheric symmetry As mentioned in section 2 we assume that the conductivity along the magnetic field line is very large, thus conjugate foot points are equipotential. To get a symmetric potential pattern we add the conductances and wind driven current densities of the two hemispheres together and solve for only one. The symmetry of the potential pattern is only valid at low– and mid–latitudes with closed field lines. At high latitudes the electric potential is specially treated as discussed in section 7.

The added together values from the northern and southern hemisphere are denoted by $(\cdot)^T$ (see equation (33)–(38)). In the source code in `subroutine dynamo` the following values are calculated

$$\Sigma^T_{\phi\phi}(0) = \Sigma^{NH}_{\phi\phi}(0) + \Sigma^{SH}_{\phi\phi}(0) \tag{142}$$

$$\Sigma^T_{\lambda\lambda}(0) = \Sigma^{NH}_{\lambda\lambda}(0) + \Sigma^{SH}_{\lambda\lambda}(0) \tag{143}$$

$$-\Sigma^T_C(0) = -(\Sigma^{NH}_C(0) - \Sigma^{SH}_C(0)) \tag{144}$$

$$\Sigma^T_H(0) = \Sigma^{NH}_H(0) - \Sigma^{SH}_H(0) \tag{145}$$

$$K^{DT}_{m\phi}(0) = K^{D,NH}_{m\phi}(0) + K^{D,SH}_{m\phi}(0) \tag{146}$$

$$K^{DT}_{m\lambda}(0) = K^{D,NH}_{m\lambda}(0) - K^{D,SH}_{m\lambda}(0) \tag{147}$$

Note that in the source code $-\Sigma^T_C(0)$ is put into ZIGMC, and that $-K^{D,SH}_{m\lambda}(0)$ was saved in RIM(2). The hemispherically added values are saved in the latitude indices of the northern hemisphere from $(nmlat+1)/2$, which is the index for the equator, to the pole at $nmlat$. The number of magnetic latitudes is $nmlat$.

Differencing of the right hand side In `subroutine rhspde` the right hand side is differentiated.

$$rhs = \frac{R_0}{cos\lambda_0}\left[\frac{\partial K^{DT}_{m\phi}(0)}{\partial\phi_0} + \frac{\partial K^{DT}_{m\lambda}(0)cos\lambda_0}{\partial|\lambda_0|}\right] \tag{148}$$

A central differencing scheme is used which leads to the derivative at the location $\phi(i)$, $\lambda_0(j)$

$$\begin{aligned} rhs(i,j) = &\frac{R_0}{2\Delta\phi cos\lambda_0(j)}\left[K^{DT}_{m\phi}(0)(i+1,j) - K^{DT}_{m\phi}(0)(i-1,j)\right] + \\ &\frac{R_0}{2\Delta\lambda_0 cos\lambda_0(j)}\left[K^{DT}_{m\lambda}(0)(i,j+1)cos\lambda_0(j+1) - \right. \\ &\left. K^{DT}_{m\lambda}(0)(i,j-1)cos\lambda_0(j-1)\right] \end{aligned} \tag{149}$$

with i, j the longitudinal and latitudinal index and the adjacent grid points $i\pm 1$,$j\pm 1$. The polar derivative is approximated by

$$rhs(i,j_{pole}) = -\frac{2R_0}{cos\lambda_0(j-1)mlon}\left[\sum_{i=1}^{mlon} K^{DT}_{m\lambda}(0)(i,j_{pole}-1)\right] \tag{150}$$

At the magnetic equator the northward current $K_{m\lambda}$ has to vanish see equation (109) or in [Rich95] eq. (5.30) or (5.31). Therefore the right hand side derivatives are discretized by

$$
\begin{aligned}
rhs(i, j_{eq}) =& \frac{R_0}{\Delta\phi cos\lambda_0(j_{eq})}\left[K_{m\phi}^{D,modT}(0)(i+\frac{1}{2}, j_{eq}) - K_{m\phi}^{D,modT}(0)(i-\frac{1}{2}, j_{eq})\right]+ \\
& \frac{2R_0}{\Delta\lambda_0}\left[K_{m\lambda}^{DT}(0)(i, j_{eq}+\frac{1}{2})cos\lambda_0(j_{eq}+\frac{1}{2})\right]
\end{aligned} \tag{151}
$$

with $K_{m\phi}^{D,mod}$ the modified height integrated eastward current density due to neutral winds $K_{m\phi}^{D}$, see equation (114). It is referred to section 10 eq. (171)–(173) for explanation of the discrete boundary condition at the magnetic equator. At the geomagnetic equator $cos\lambda_0(j_{eq}) = 1$ and equation (151) can be written as

$$
\begin{aligned}
rhs(i, j_{eq}) =& \frac{R_0}{2\Delta\phi_0}\left[K_{m\phi}^{D,modT}(0)(i+1, j_{eq}) - K_{m\phi}^{D,modT}(0)(i-1, j_{eq})\right]+ \\
& \frac{R_0}{\Delta\lambda_0}\left[K_{m\lambda}^{DT}(0)(i, j_{eq}+1)cos\lambda_0(j_{eq}+1) + K_{m\lambda}^{DT}(0)(i, j_{eq})\right]
\end{aligned} \tag{152}
$$

The whole right hand side is multiplied by R_0 in [m] to get eq. (148).

Differencing of the left hand side In this paragraph the finite differencing of the left hand side of the electrodynamo equation is discussed. In the source code the calling tree for the differencing is the following:

```
subroutine dynamo
...
if (isolve == 2) then
   call stencmd
        call htrpex
        call cnmmod
        call cnm
else
   call stencil
        call htrpex
        call cnm
endif
...
```

The flag isolve=2 means that at the finest grid level an additional coefficient matrix is set up without upwinding for terms violating the diagonal dominance (see paragraph further down in this section). The multigrid solver which is discussed in section 11 uses the coefficient matrix without upwinding to calculate the residual on the finest grid level. At all other grid levels the coefficient matrix with upwinding is used to solve for the residual. If isolve$\neq$ 2 the upwinding method is applied at all grid levels to solve for the electric potential. For more information about the different option with the multigrid solver we refer to section 11.

In `subroutine dynamo` the conductances are prepared for the finite differencing. The conductance coefficients represent

$$A = \frac{\Sigma^T_{\phi\phi}(0)}{cos\lambda_0 \Delta\phi^2} \rightarrow zigm11 \tag{153}$$

$$B = \frac{\Sigma^T_{\lambda\lambda}(0) cos\lambda_0}{\Delta\lambda_0^2} \rightarrow zigm22 \tag{154}$$

$$C = \frac{\Sigma^T_{\phi\lambda}(0)}{4\Delta\lambda_0 \Delta\phi} \rightarrow zigmc \tag{155}$$

$$D = \frac{\Sigma^T_{\phi\lambda}(0)}{4\Delta\lambda_0 \Delta\phi} \rightarrow zigm2 \tag{156}$$

with `zigm11`, `zigm22`, `zigmc`, `zigm2` the variable names in the source code. Note that the factor of four is introduced due to the central differencing. Both hemisphere are already added together and the coefficients are stored in the index range of the "northern hemisphere" ((nmlat+1)/2 to nmlat). In the "southern hemisphere" index range (1 to (nmlat+1)/2), the same values are stored as in the northern range ((nmlat+1)/2 to nmlat) except of the two mixed terms which change sign.

$$zigmc(SH) \rightarrow -\frac{\Sigma^T_{\phi\lambda}(0)}{4\Delta\lambda_0 \Delta\phi} \tag{157}$$

$$zigm2(SH) \rightarrow -\frac{\Sigma^T_{\phi\lambda}(0)}{4\Delta\lambda_0 \Delta\phi} \tag{158}$$

The polar value of $\frac{\Sigma^T_{\phi\phi}(0)}{cos\lambda_0 \Delta\phi^2}$ is set to zero to avoid floating point exception. The polar value is not used in the electrodynamo equation since the potential at the pole is prescribed.

The `subroutine stencmd` or `subroutine stencil` is called for each conductance term eq. (153)–(156) and the finite difference stencil is updated for the contributions of the corresponding conductance term. First the conductance is copied into a working array in `subroutine htrpex` and the longitudinal wrap around points, necessary for the longitudinal derivatives, are set. Note that there are 5 different grid levels and therefore there are 16 additional points on either side of the working array. The working array stores the values from the equator (index 1) to the pole (index (nmlat+1)/2).

The contributions to the stencil from the different conductances are determined in `subroutine cnmmod` and/or `subroutine cnm`. `Subroutine cnmmod` is called if the flag isolve=2 is set, and then only for the finest grid level This subroutine sets up the coefficient stencil without upwinding method. At all the other grid levels upwinding may be used if necessary. For isolve $\neq$ 2 all the stencils are determined with upwinding methods if necessary, which is done in `subroutine` `cnm`. Please read section 11 for more information about the different solver types (flag isolve).

From equation (116) and the values in table 5 we get the following left hand side of the electrodynamo equation.

$$
\begin{aligned}
cos\lambda_0 \; lhs = & \frac{\partial}{\partial \phi_0}\left(\frac{\Sigma^T_{\phi\phi}(0)}{cos\lambda_0}\frac{\partial \Phi}{\partial \phi_0} + \Sigma^T_{\phi\lambda}(0)\frac{\partial \Phi}{\partial \lambda_0}\right) + \\
& \frac{\partial}{\partial \lambda_0}\left(\Sigma^T_{\lambda\phi}(0)\frac{\partial \Phi}{\partial \phi_0} + \Sigma^T_{\lambda\lambda}(0) cos\lambda_0 \frac{\partial \Phi}{\partial \lambda_0}\right)
\end{aligned}
\tag{159}
$$

Note that the right hand side rhs in equation (148) is already divided by $cos\lambda_0$ therefore we have to include the $cos\lambda_0$ on the left hand side of eq. (159). Replacing the two terms in the brackets in eq. (159) by

$$
T_\phi = \frac{\Sigma^T_{\phi\phi}(0)}{cos\lambda_0}\frac{\partial \Phi}{\partial \phi_0} + \Sigma^T_{\phi\lambda}(0)\frac{\partial \Phi}{\partial \lambda_0} \tag{160}
$$

$$
T_\lambda = \Sigma^T_{\lambda\phi}(0)\frac{\partial \Phi}{\partial \phi_0} + \Sigma^T_{\lambda\lambda}(0) cos\lambda_0 \frac{\partial \Phi}{\partial \lambda_0} \tag{161}
$$

leads to

$$
cos\lambda_0 \; lhs = \frac{\partial}{\partial \phi_0} T_\phi + \frac{\partial}{\partial \lambda_0} T_\lambda \tag{162}
$$

For clarity we will omit the dependence on λ_0 shown by $(\cdot)(0)$ in the following e.g. we write $\Sigma^T_{\phi\lambda}$ instead off $\Sigma^T_{\phi\lambda}(0)$. Using central differencing for the finite differences gives

$$
cos\lambda_0 \; lhs = \frac{T_\phi(i+\frac{1}{2}, j) - T_\phi(i-\frac{1}{2}, j)}{\Delta \phi_0} + \frac{T_\lambda(i, j+\frac{1}{2}) - T_\lambda(i, j-\frac{1}{2})}{\Delta \lambda_0} \tag{163}
$$

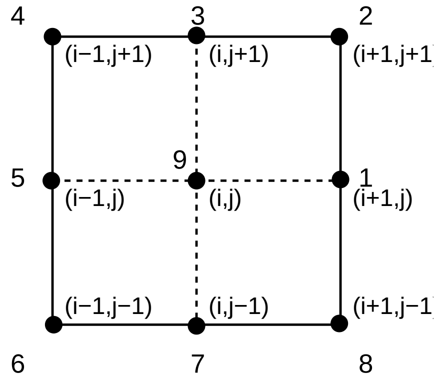

Figure 5: Geometry for the 9 point stencil

with

$$
\begin{aligned}
T_\phi(i+\frac{1}{2},j) =& \frac{\Sigma^T_{\phi\phi}(i+\frac{1}{2},j)}{cos\lambda_0(j)}\frac{\Phi(i+1,j)-\Phi(i,j)}{\Delta\phi_0}+\\
&\Sigma^T_{\phi\lambda}(i+\frac{1}{2},j)\frac{\Phi(i+\frac{1}{2},j+\frac{1}{2})-\Phi(i+\frac{1}{2},j-\frac{1}{2})}{\Delta\lambda_0}\\
T_\phi(i-\frac{1}{2},j) =& \frac{\Sigma^T_{\phi\phi}(i-\frac{1}{2},j)}{cos\lambda_0(j)}\frac{\Phi(i,j)-\Phi(i-1,j)}{\Delta\phi_0}+\\
&\Sigma^T_{\phi\lambda}(i-\frac{1}{2},j)\frac{\Phi(i-\frac{1}{2},j+\frac{1}{2})-\Phi(i-\frac{1}{2},j-\frac{1}{2})}{\Delta\lambda_0}\\
T_\lambda(i,j+\frac{1}{2}) =& \Sigma^T_{\lambda\phi}(i,j+\frac{1}{2})\frac{\Phi(i+\frac{1}{2},j+\frac{1}{2})-\Phi(i-\frac{1}{2},j+\frac{1}{2})}{\Delta\phi_0}+\\
&\Sigma^T_{\lambda\lambda}(i,j+\frac{1}{2})cos\lambda_0(j+\frac{1}{2})\frac{\Phi(i,j+1)-\Phi(i,j)}{\Delta\lambda_0}\\
T_\lambda(i,j-\frac{1}{2}) =& \Sigma^T_{\lambda\phi}(i,j-\frac{1}{2})\frac{\Phi(i+\frac{1}{2},j-\frac{1}{2})-\Phi(i-\frac{1}{2},j-\frac{1}{2})}{\Delta\phi_0}+\\
&\Sigma^T_{\lambda\lambda}(i,j-\frac{1}{2})cos\lambda_0(j-\frac{1}{2})\frac{\Phi(i,j)-\Phi(i,j-1)}{\Delta\lambda_0}
\end{aligned}
\tag{164}
$$

The numbering of the nine point stencil can be seen in figure 5 with the index i denoting the longitude and the index j for the latitude. The values at half grid points e.g. $(i+\frac{1}{2},j)$ are determined by averaging the values of the adjacent grid points, e.g.

$$\Sigma^T_{\phi\phi}(i+\frac{1}{2},j) = \frac{1}{2}\left[\Sigma^T_{\phi\phi}(i+1,j)+\Sigma^T_{\phi\phi}(i,j)\right] \tag{165}$$

Accordingly, the values at $(i-\frac{1}{2},j)$, $(i,j+\frac{1}{2})$ and $(i,j-\frac{1}{2})$ can be calculated. The difference at half points in latitude and longitude e.g. $(i+\frac{1}{2},j+\frac{1}{2})$ is also resolved by averaging the values of the adjacent grid points which leads to e.g.

$$\begin{aligned}&\Phi(i+\frac{1}{2},j+\frac{1}{2})-\Phi(i+\frac{1}{2},j-\frac{1}{2})=\\&\frac{1}{4}\big[\Phi(i+1,j+1)-\Phi(i+1,j-1)+\Phi(i,j+1)-\Phi(i,j-1)\big]\end{aligned}\tag{166}$$

Accordingly, $\Phi(i-\frac{1}{2},j+\frac{1}{2})-\Phi(i-\frac{1}{2},j-\frac{1}{2})$, $\Phi(i+\frac{1}{2},j+\frac{1}{2})-\Phi(i-\frac{1}{2},j+\frac{1}{2})$ and $\Phi(i+\frac{1}{2},j-\frac{1}{2})-\Phi(i-\frac{1}{2},j-\frac{1}{2})$ are discretized. The resulting contributions from the conductance terms to the nine point stencil in figure 5 are summarized in table 6. Therein, we are using the abbreviations A, B, C, D from equations (153)–(156) for the conductance quantities.

Upwinding In the following the contributions to the stencil are denotes by the variable c, e.g. at node 9 the coefficient would be c(i,j). The stability is not preserved if the stencil coefficient of adjacent points of c(i,j) are changing sign e.g. $c(i+1,j)c(i-1,j)<0$ or $c(i,j+1)c(i,j-1)<0$. To avoid instabilities the diagonal dominance of the coefficient matrix has to be preserved. This can be done by using upwinding methods depending on the orientation of the flux (i.e. the sign of the stencil coefficients). The derivatives with respect to e.g. λ_0 for the central differencing is

$$\frac{d\Phi(i+\frac{1}{2},j)}{d\lambda_0}=\frac{1}{\Delta\lambda_0}\big[\Phi(i+\frac{1}{2},j+\frac{1}{2})-\Phi(i+\frac{1}{2},j-\frac{1}{2})\big]\tag{167}$$

and the upwinding leads to

$$\begin{aligned}\frac{d\Phi(i+\frac{1}{2},j)}{d\lambda_0}&=\frac{1}{2}\big[\frac{d\Phi(i+1,j)}{d\lambda_0}+\frac{d\Phi(i,j)}{d\lambda_0}\big]\\&=\frac{1}{2}\big[\frac{\Phi(i+1,j+1)-\Phi(i+1,j-1)}{2\Delta\lambda_0}+\frac{\Phi(i,j+1)-\Phi(i,j)}{\Delta\lambda_0}\big]\\\frac{d\Phi(i+\frac{1}{2},j)}{d\lambda_0}&=\frac{1}{2}\big[\frac{d\Phi(i+1,j)}{d\lambda_0}+\frac{d\Phi(i,j)}{d\lambda_0}\big]\\&=\frac{1}{2}\big[\frac{\Phi(i+1,j+1)-\Phi(i+1,j-1)}{2\Delta\lambda_0}+\frac{\Phi(i,j)-\Phi(i,j-1)}{\Delta\lambda_0}\big]\end{aligned}\tag{168}$$

and for the derivative with respect to longitude ϕ the upwinding results in

$$\begin{aligned}\frac{d\Phi(i,j+\frac{1}{2})}{d\phi_0}&=\frac{1}{2}\big[\frac{d\Phi(i,j+1)}{d\phi_0}+\frac{d\Phi(i,j)}{d\phi_0}\big]\\&=\frac{1}{2}\big[\frac{\Phi(i+1,j+1)-\Phi(i-1,j+1)}{\Delta\phi_0}+\frac{\Phi(i+1,j)-\Phi(i,j)}{2\Delta\phi_0}\big]\\\frac{d\Phi(i,j+\frac{1}{2})}{d\phi_0}&=\frac{1}{2}\big[\frac{d\Phi(i,j+1)}{d\phi_0}+\frac{d\Phi(i,j)}{d\phi_0}\big]\\&=\frac{1}{2}\big[\frac{\Phi(i+1,j+1)-\Phi(i-1,j+1)}{2\Delta\phi_0}+\frac{\Phi(i,j)-\Phi(i-1,j)}{\Delta\phi_0}\big]\end{aligned}\tag{169}$$

node	$A = \frac{\Sigma^T_{\phi\phi}}{\Delta\phi^2 cos\lambda_0}$	$B = \frac{\Sigma^T_{\lambda\lambda}(0) cos\lambda_0}{\Delta\lambda_0^2}$	$C = \frac{\Sigma^T_{\phi\lambda}(0)}{4\Delta\lambda_0\Delta\phi}$	$D = \frac{\Sigma^T_{\lambda\phi}(0)}{4\Delta\lambda_0\Delta\phi}$
1	$A(i+\frac{1}{2},j)$	-	-	$D(i,j+\frac{1}{2}) - D(i,j-\frac{1}{2})$
2	-	-	$C(i+\frac{1}{2},j)$	$D(i,j+\frac{1}{2})$
3	-	$B(i,j+\frac{1}{2})$	$C(i+\frac{1}{2},j) - C(i-\frac{1}{2},j)$	-
4	-	-	$-C(i-\frac{1}{2},j)$	$-D(i,j+\frac{1}{2})$
5	$A(i-\frac{1}{2},j)$	-	-	$-D(i,j+\frac{1}{2}) + D(i,j-\frac{1}{2})$
6	-	-	$C(i-\frac{1}{2},j)$	$D(i,j-\frac{1}{2})$
7	-	$B(i,j-\frac{1}{2})$	$-C(i+\frac{1}{2},j) + C(i-\frac{1}{2},j)$	-
8	-	-	$-C(i+\frac{1}{2},j)$	$-D(i,j-\frac{1}{2})$
9	$-A(i+\frac{1}{2},j) - A(i-\frac{1}{2},j)$	$-B(i,j+\frac{1}{2}) - B(i,j-\frac{1}{2})$	-	-

Table 6: Contributions from conductance terms to nine point stencil using central differencing for all terms (see `subroutine cnm` and `subroutine cnmmod`)

node	$C = \frac{\Sigma^T_{\phi\lambda}(0)}{4\Delta\lambda_0\Delta\phi}$	$D = \frac{\Sigma^T_{\phi\lambda}(0)}{4\Delta\lambda_0\Delta\phi}$
1	-	$2D(i,j+\frac{1}{2}) - 2D(i,j-\frac{1}{2})$
3	$2C(i+\frac{1}{2},j) - 2C(i-\frac{1}{2},j)$	-
5	-	-
7	-	-
9	$-2C(i+\frac{1}{2},j) + 2C(i+\frac{1}{2},j)$	$-2D(i,j+\frac{1}{2}) + 2D(i,j-\frac{1}{2})$

Table 7: Modification to stencil due to upwinding with positive flux $f_l > 0$ in `subroutine cnm` and `subroutine cnmmod`

node	$C = \frac{\Sigma^T_{\phi\lambda}(0)}{4\Delta\lambda_0\Delta\phi}$	$D = \frac{\Sigma^T_{\phi\lambda}(0)}{4\Delta\lambda_0\Delta\phi}$
1	-	-
3	-	-
5	-	$-2D(i,j+\frac{1}{2}) + 2D(i,j-\frac{1}{2})$
7	$-2C(i+\frac{1}{2},j) + 2C(i-\frac{1}{2},j)$	-
9	$2C(i+\frac{1}{2},j) - 2C(i+\frac{1}{2},j)$	$2D(i,j+\frac{1}{2}) - 2D(i,j-\frac{1}{2})$

Table 8: Modification to stencil due to upwinding with negative flux $f_l < 0$ in `subroutine cnm` and `subroutine cnmmod`

The flux at the center of the stencil (i, j) is determined by the flux average of the two adjacent points in the corresponding direction. Thus, the latitudinal flux at the center c(i,j) is $f_l = \frac{1}{2}[c(i,j+1) + c(i,j-1)]$ and the longitudinal flux is $f_l = \frac{1}{2}[c(i+1,j) + c(i-1,j)]$. For positive flux $f_l > 0$ the values in table 7 are used and for negative flux $f_l < 0$ the modifications in table 8 are applied. If the flux at the two adjacent points goes into the same direction $c(i+1,j)c(i-1,j) > 0$ or $c(i,j+1)c(i,j-1) > 0$ the central differencing in table 6 is used.

Equatorial boundary At the equator the coefficient stencil has to be modified to take into account the boundary condition which was described in section 8 eq. (109)–(114). The discrete modification to the right hand side was described in the paragraph on page 30 eq. (151) but the derivation will be explained in the following together with the left hand side.
Including the equatorial boundary condition eq. (109) into the electrodynamo equation eq. (32) leads to eq. (112). The boundary condition can be rewritten as

$$\Sigma_{\lambda\phi}\frac{\partial\Phi}{\partial\phi_m} + \Sigma_{\lambda\lambda}cos\lambda_m\frac{\partial\Phi}{\partial|\lambda_m|} = R_0 cos\lambda_m K^D_{m\lambda} \tag{170}$$

and from which in discrete form follows that

$$\begin{aligned} T_\lambda(i,j_{eq}+\frac{1}{2}) + T_\lambda(i,j_{eq}-\frac{1}{2}) =& R_0 cos\lambda_0(j_{eq}+\frac{1}{2})K^D_{m\lambda}(i,j_{eq}+\frac{1}{2}) + \\ & R_0 cos\lambda_0(j_{eq}-\frac{1}{2})K^D_{m\lambda}(i,j_{eq}-\frac{1}{2}) \end{aligned} \tag{171}$$

node	$A = \frac{\Sigma^T_{\phi\phi}}{\Delta\phi^2 cos\lambda_0}$	$B = \frac{\Sigma^T_{\lambda\lambda}(0) cos\lambda_0}{\Delta\lambda_0^2}$	$C = \frac{\Sigma^T_{\phi\lambda}(0)}{4\Delta\lambda_0\Delta\phi}$	$D = \frac{\Sigma^T_{\phi\lambda}(0)}{4\Delta\lambda_0\Delta\phi}$
1	$A(i+\frac{1}{2},j)$	-	-	$D(i,j+\frac{1}{2})$
2	-	-	-	$D(i,j+\frac{1}{2})$
3	-	$B(i,j+\frac{1}{2})$	-	-
4	-	-	-	$-D(i,j+\frac{1}{2})$
5	$A(i-\frac{1}{2},j)$	-	-	$-D(i,j+\frac{1}{2})$
6	-	-	-	-
7	-	-	-	-
8	-	-	-	-
9	$-A(i+\frac{1}{2},j)-A(i-\frac{1}{2},j)$	$-B(i,j+\frac{1}{2})$	-	-

Table 9: Modification to stencil at the equator (see `subroutine cnm` or `subroutine cnmmod`)

with T_λ defined in eq. (161). The electrodynamo equation at the equator (112)) is discretizied by

$$\frac{1}{cos\lambda_0(j_{eq})}\left[\frac{T_\phi(i+\frac{1}{2},j_{eq})-T_\phi(i-\frac{1}{2},j_{eq})}{\Delta\phi_0}+\frac{T_\lambda(i,j_{eq}+\frac{1}{2})-T_\lambda(i,j_{eq}-\frac{1}{2})}{\Delta\lambda_0}\right]=$$
$$\frac{R_0}{cos\lambda_0(j_{eq})\Delta\phi_0}\left[K^{D,modT}_{m\phi}(i+\frac{1}{2},j_{eq})-K^{D,modT}_{m\phi}(i-\frac{1}{2},j_{eq})\right]+$$
$$\frac{R_0}{cos\lambda_0(j_{eq})\Delta\lambda_0}\left[K^{DT}_{m\lambda}(i,j_{eq}+\frac{1}{2})cos\lambda_0(j_{eq}+\frac{1}{2})-K^{DT}_{m\lambda}(i,j_{eq}-\frac{1}{2})cos\lambda_0(j_{eq}-\frac{1}{2})\right] \quad (172)$$

Inserting equation (171) into the electrodynamo equation (172) the values $K^{DT}_{m\lambda}(i,j_{eq}-\frac{1}{2})$ and $T_\lambda(i,j_{eq}-\frac{1}{2})$ are substituted by $K^{DT}_{m\lambda}(i,j_{eq}+\frac{1}{2})$ and $T_\lambda(i,j_{eq}+\frac{1}{2})$ which lead to

$$fracT_\phi(i+\frac{1}{2},j_{eq})-T_\phi(i-\frac{1}{2},j_{eq})\Delta\phi_0+\frac{2T_\lambda(i,j_{eq}+\frac{1}{2})}{\Delta\lambda_0}=$$
$$\frac{R_0}{\Delta\phi_0}\left[K^{D,modT}_{m\phi}(i+\frac{1}{2},j_{eq})-K^{D,modT}_{m\phi}(i-\frac{1}{2},j_{eq})\right]+ \quad (173)$$
$$\frac{R_0}{\Delta\lambda_0}\left[2K^{DT}_{m\lambda}(i,j_{eq}+\frac{1}{2})cos\lambda_0(j_{eq}+\frac{1}{2})\right]$$

with $cos\lambda_0(j_{eq})=1$ and the value $T_\phi=\frac{\Sigma^{modT}_{\phi\phi}(0)}{cos\lambda_0}\frac{\partial\Phi}{\partial\phi_0}$ at the equator. Therefore the stencil has to be modified at the equator according to table 9 with $B(i,j-\frac{1}{2})=0$, $D(i,j-\frac{1}{2})=0$ and no $\Sigma_{\phi\lambda}$ contributions. The coefficients for A are not changing (see table 6).

Coefficient stencil In table 10 the longitudinal and latitudinal dimensions of the 5 different grid levels are given. On the finest grid level the right hand side

grid level	variable c^*	long.dimension	lat.dimension $nmlat^*$	"points" of stencil
0	c0	81	49	10
1	c1	41	25	9
2	c2	21	13	9
3	c3	11	7	9
4	c4	6	4	9

Table 10: Coefficient matrix name and dimensions at the different grid levels

is stored in $c0(:,:,10)$. Therefore the dimension is 10 instead of 9, which is the size at all other grid levels. At the pole ($j = nmlat^*$) the off diagonal terms are set to zero and the diagonal terms to one $c^*(i, nmlat^*, 9) = 1$ in `subroutine edges` with $(\cdot)^*$ denoting the different grid levels. The right hand side is set to one at the pole $c0(i, nmlat, 10) = 1$. The left hand side lhs is finally divided by $cos\lambda_0$ in `subroutine divide`.

11 Solving for the electric potential

In TIEGCM a multigrid solver is used which was developed by J. Adams. The source code and information can be found at http://www.scd.ucar.edu-/css/software/mudpack/. In the original mudpack solver the finite differencing and the setting of all the boundary conditions are part of solver package. For TIEGCM the stencil and the boundary conditions are already set up in the TIEGCM code, and therefore the multigrid solver was modified accordingly. We have three different solver options in TIEGCM which are all based on the mudpack multigrid package.

- isolve=0 multigrid solver `mudcr2` (see section 11.1)
- isolve=1 multigrid solver `muhcr2` as direct solver (see section 11.2)
- isolve=2 modified multigrid solver `mudcr2` (see section 11.3)

11.1 Multigrid solver `mudcr2`

The `subroutine mud2cr` attempts to compute the second-order difference approximation to a two-dimensional linear nonseparable elliptic partial differential equation with cross derivative terms on a rectangle. The approximation is generated on a uniform grid covering the rectangle. The parameters used for the multigrid solver in TIEGCM are the following:

- intl=0: this is an input to the subroutine and is zero for the initial call to `mud2cr` to check for errors. After the initial call of `mud2cr` intl=1 will be set and the PDE is solved.
- boundary conditions: with x being the longitudinal direction and y the latitudinal one from the equator to the pole.
  - nxa =0 : flags boundary conditions on the edge x=xa. nxa = 0 means the boundary condition is periodic in x on [xa,xb].
  - nxb =0: flags boundary conditions on the edge x=xb. nxb = 0 means the boundary condition is periodic in x on [xa,xb].
  - nyc =2: flags boundary conditions on the edge y=yc (equator). nyc = 2 means that there are mixed derivative boundary conditions at y=yc.
  - nyd =1: flags boundary conditions on the edge y=yd (pole). nyd=1 means that the boundary condition is specified and input thru the variable `phi`.
- defining the number of grid points in x (longitude) and y (latitude) direction
  - ixp = 5: ixp+1 is the number of points on the coarsest x grid visited during multigrid cycling.

- jyq = 3: jyq+1 is the number of points on the coarsest y grid visited during multigrid cycling.
- iex = 5: integer exponent of 2 used in defining the number of grid points in the x direction
- jey = 5: integer exponent of 2 used in defining the number of grid points in the y direction
- nx: number of equally spaced grid points in the interval [xa,xb] $nx = ixp\ 2^{iex-1} + 1$
- ny: number of equally spaced grid points in the interval [yc,yd] $ny = jyq\ 2^{jey-1} + 1$

- iguess = 0: no initial guess is used forcing full multigrid cycling
- tolmax = 0.01: tolmax is the maximum relative error tolerance used to terminate the relaxation iterations. Assume Φ_1 and Φ_2 are the last two computed approximations at the finest grid level. If we define $\Phi_{diff} = max(|\Phi_2(i,j) - \Phi_1(i,j)|)$ for all i,j and $\Phi_{max} = max(|\Phi_2(i,j)|)$ for all i,j then convergence is considered to have occurred if and only if $\frac{\Phi_{diff}}{\Phi_{max}} < tolmax$
- maxcy = 150: if $tolmax > 0.0$ is input, which means error control is used, then maxcy is the limit on the number of cycles between the finest and coarsest grid levels. When the multigrid iteration is working correctly only a few cycles are required for convergence.
- method = 3: method of relaxation. If neither fx (the longitudinal second order derivative $\Sigma_{\phi\phi}/\Delta\phi^2$) or fy (the latitudinal second order derivative $\Sigma_{\lambda\lambda}/\Delta\lambda_0^2$) dominates over the solution region and they both vary considerably choose method = 3, which uses line relaxation in both the x and y direction
- nwork: length of work array
  $length = [7(nx+2)(ny+2) + 4(11 + isx + jsy)nx * ny]/3$
- mgopt: multigrid options the default values (2,2,1,3) in the vector `mgopt` were chosen for robustness.
  - mgopt(1) = 2: w cycling
  - mgopt(2) = 2: the number of pre–relaxation sweeps executed before the residual is restricted and cycling is invoked at the next coarser grid level
  - mgopt(3) = 1: the number of post–relaxation sweeps executed after the cycling has been invoked at the next coarser grid level and the residual correction has been transferred back
  - mgopt(4) = 3: multicubic prolongation (interpolation) is used to transfer residual corrections and the PDE approximation from the coarse to the fine grid within full multigrid cycling.

- output Φ: solution of PDE which is the electric potential
- output ierror: indicates invalid input arguments when returned positive and nonfatal warnings when returned negative.

If no convergence is reached with this version of the multigrid solver the direct solver described in section 11.2 is used.

11.2 Multigrid solver `muhcr2` as direct solver

This solver which is in `subroutine muh2cr` is originally a hybrid multigrid/direct method which approximates the same 2-d nonseparable elliptic PDE as the mudpack solver `mud2cr`. Using a direct method combines the efficiency of multigrid iteration with the certainty of a direct method. The basic algorithm is modified by using banded Gaussian elimination in place of relaxation whenever the coarsest subgrid is encountered within the multigrid cycling. The solver becomes a full direct method if grid size arguments are chosen so that the coarsest and finest grids coincide, i.e. choosing iex=jey=1 and ixp=nx-1, jyq=ny-1. This will set the Gaussian elimination on the finest grid. In this case, `subroutine muh2cr` produces a direct solution to the same nonseparable elliptic PDE. In TIEGCM we are using the solver `muhcr2` only as a direct solver.

11.3 Modified multigrid solver `mudcr2`

This solver is the same as the solver in section 11.1 only with the exception that the residual is calculated with the coefficient stencil without upwinding (see section 10). Therefore the solution converges toward the solution of the direct solver using the coefficient stencil without the upwinding method. In general upwinding introduces unwanted numerical dissipation. The unmodified coefficient stencil is stored in the array `cofum`. In comparison with the solver in section 11.1 the number of relaxation steps has to be increased to get convergence.

- mgopt(2) = 3: the number of pre–relaxation sweeps executed before the residual is restricted and cycling is invoked at the next coarser grid level
- mgopt(3) = 2: the number of post–relaxation sweeps executed after cycling has been invoked at the next coarser grid level and the residual correction has been transferred back

All the other parameters remain the same and can be found in section 11.1. If no convergence is reached with this multigrid solver the direct solver described in section 11.2 is called.

12 Electric Field

In `subroutine threed` the two and three dimensional electric field and the three dimensional electric potential is calculated from the two dimensional electric potential Φ. The components of the electric field E_{d1} and E_{d2} which are in more-or-less magnetic eastward and downward/equatorward direction are determined by

$$E_{d1} = -\frac{1}{R_0 cos\lambda_m}\frac{\partial\Phi}{\partial\phi_m} \tag{174}$$

$$E_{d2} = \frac{1}{R_0 sinI_m}\frac{\partial\Phi}{\partial\lambda_m} \tag{175}$$

In the code the equally spaced latitudinal grid point distribution λ_0 in λ_m^* is used to calculate the derivatives. Therefore the mapping factors from the irregular latitudinal spaced grid λ_m^* to λ_0 have to be taken into account. Including these factors the discrete derivatives are

$$E_{d1}(i,j) = -\frac{1}{R_0}\frac{cos\lambda_0(j)}{cos\lambda_m^*(j)}\frac{\Phi(i-1,j)-\Phi(i+1,j)}{2cos\lambda_0(j)\Delta\phi_m} \tag{176}$$

$$E_{d2}(i,j) = \frac{1}{R_0}\frac{\partial\lambda_0(j)}{|sinI_m(j)|\partial\lambda_m^*(j)}\frac{\Phi(i,j-1)-\Phi(i,j+1)}{2\Delta\lambda_0} \tag{177}$$

The polar values are averaged over the four surrounding points. At the equator a second order polynomial of the electric potential is fitted through the adjacent points and thus the derivative of the polynomial at the equator is determined.

The three dimensional electric potential and electric field is calculated assuming that the dipolar magnetic field lines are equipotential. At each grid point $(\phi(i), \lambda_m^*(j), h(k))$ the foot point of the magnetic field line going through this grid point is determined. Having found the foot point of the field line at height h_0 the values, i.e. electric potential and electric field, at this point can be determined by a two dimensional interpolation of the surrounding points. The polar values are determined by longitudinal averaging all the polar values.

13 Additional features

13.1 Magnetic perturbations

The magnetic perturbation from a TIEGCM model run can be determined by using the postprocessor program `MagIon`. The program is available upon request together a `MagIon` user guide, a model description is in preparation. The global magnetic perturbations at the ground and above the ionosphere at low orbiting satellite heights can be determined, or what a magnetometer would measure at the ground. For details about the calculation and the necessary assumption we refer to [Rich05], [Rich74] and the `MagIon` user guide.

To calculate the magnetic perturbation the radial component of the field-aligned current J_{qr} and the height–integrated current densities $K_{m\phi}$ and $K_{m\lambda}$ have to be known. In addition, if the influence of gravity and plasma pressure gradient driven current should be included the height dependent $K_{m\phi}^{int}$ have to be determined with and without the current driven by gravity and plasma pressure gradient. The calculation of these currents is not the default in the TIEGCM source code, thus the flag icalkqlam $==1$ in the `module dynamo` has to be set. In the following the calculation of the different currents J_{qr}, $K_{q\phi}$ and $K_{q\lambda}$, which can be found in the file `current.F`, is described.

13.1.1 Field–aligned current J_{qr}

The field–aligned current can be determined from the electrodynamo equation (32) without the assumption of symmetrical hemispheres which leads to

$$\begin{aligned}
&\frac{\partial}{\partial \phi_m}\left(\frac{\Sigma_{\phi\phi}}{cos\lambda_m}\frac{\partial \Phi}{\partial \phi_m}+\Sigma_{\phi\lambda}\frac{\partial \Phi}{\partial |\lambda_m|}\right)+\frac{\partial}{\partial |\lambda_m|}\left(\Sigma_{\lambda\phi}\frac{\partial \Phi}{\partial \phi_m}+\Sigma_{\lambda\lambda}cos\lambda_m\frac{\partial \Phi}{\partial |\lambda_m|}\right)\\
&= R\frac{\partial K_{m\phi}^D}{\partial \phi_m}+R\frac{\partial K_{m\lambda cos\lambda_m}^D}{\partial |\lambda_m|}+R^2 cos\lambda_m J_{mr}
\end{aligned} \tag{178}$$

Note that compared to the electrodynamo equation (32) the conductances and the wind driven current are different in the northern and southern hemisphere denoted by e.g. $\Sigma_{\phi\phi}$ instead of $\Sigma_{\phi\phi}^T$. Therefore we determine the finite difference coefficient stencil for both hemispheres instead of only one as described in section 10 on page 31. The set up of the finite difference stencil is analog to the one for only one hemisphere. The `subroutine nosocoef` sets up the coefficient stencil for both hemisphere and also saves the wind driven current. The `subroutine nosocoef` is called shortly after the field line integrations i.e. before the conductances and wind driven currents are added together from the two hemispheres (see table 5). The conductances are prepared for the finite differencing and represent

$$A = \frac{\Sigma_{\phi\phi}(0)}{cos\lambda_0 \Delta\phi^2} \rightarrow nszigm11 \tag{179}$$

$$B = \frac{\Sigma_{\lambda\lambda}^{(}0) cos\lambda_0}{\Delta\lambda_0^2} \rightarrow nszigm22 \tag{180}$$

$$C = \frac{\Sigma_{\phi\lambda}(0)}{4\Delta\lambda_0 \Delta\phi} \rightarrow nszigmc \tag{181}$$

$$D = \frac{\Sigma_{\phi\lambda}(0)}{4\Delta\lambda_0 \Delta\phi} \rightarrow nszigm2 \tag{182}$$

The set up of the stencil is analog to section 10 see table 6 and 9 with A, B, C and D from the definitions above eq. (179)–(182).

The calling tree is

```
...
call nsstencil
   call nscnm
...
```

Note that the stencil is only calculated on the finest grid. In addition no upwinding method to preserve the diagonal dominance is used since the finite difference stencil is not used for solving. The numbering of the nine node stencil for the southern hemisphere is the same as for the northern hemisphere, which is illustrated in figure 6 for both hemispheres. This means that e.g. points 6", 7" and 8" in the southern hemisphere are toward the poles and not toward the equator as for the northern hemisphere points 6, 7 and 8. This switch of the nodes 6, 7, 8 with 4, 3, 2 is reflected in the set up of the stencil in the southern hemisphere done in `subroutine nscnm`. The result is stored in the array `nscoef`. The wind driven currents of the right hand side are treated in the same way as in the dynamo equation in section 10 on page 30. The right hand side is saved in the array `nsrhs`.

Having set up the finite difference coefficient matrix $\bar{\mathbf{C}}$ of the left hand side, as described in the previous paragraph, and determined the wind driven current of the right hand side vector **rhs** we can insert the calculated electric potential vector $\mathbf{\Phi}$ into equation (178) to solve for the field aligned current vector $\mathbf{J}_{mr}$.

$$R_0^2 \frac{cos\lambda_m}{cos\lambda_0} \frac{\partial\lambda_0}{\partial\lambda_m^*} J_{mr} = \bar{C}\Phi - \text{rhs} \tag{183}$$

Note that the whole electrodynamo equation was multiplied by $\frac{1}{cos\lambda_0}\frac{\partial\lambda_0}{\partial\lambda_m^*}$ as mentioned on page 5. The current calculation is done in `subroutine nosocrrt`. For the polar values the average values at adjacent latitudinal point are extrap-

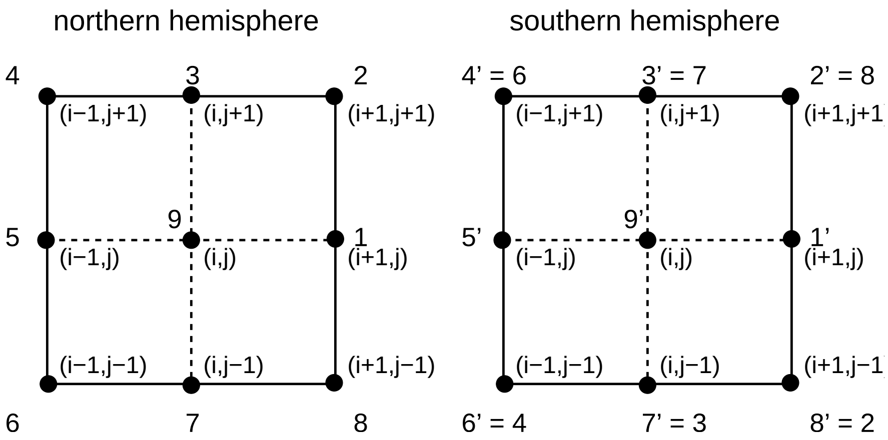

Figure 6: Geometry for the 9 point stencil in the northern and southern hemisphere

olated by

$$J_{mr}(j_{pole}) = \frac{1}{8\text{nmlon}} \left[9 \sum_{i=1}^{nmlon} J_{mr}(i, j_{pole} \mp 1) - \sum_{i=1}^{nmlon} J_{mr}(i, j_{pole} \mp 2) \right] \quad (184)$$

with $nmlon$ the number of longitudes and j_{pole} the latitudinal index at the north / south pole and the $\mp$ sign referring to the poles respectively. Close to the magnetic equator there is no distinct allocation of the current to either the height integrated current density $K_{m\lambda}$ or the field–aligned current J_{mr} since the magnetic field lines are almost horizontal in this region. Therefore the allocation to either one of the two currents $K_{m\lambda}$ and J_{mr} depends strongly on the reference height h_0. Raising the reference height will shift the current from the field line to the ionospheric current sheet $K_{m\lambda}$. The exact distribution of the current at the equator can be neglected for the calculation of the magnetic perturbations. Therefore we linearly interpolate the field–aligned current between $\pm 12^o$ latitude.

$$J_{mr}(j) = \frac{J_{mr}(\lambda_m^{max}) J_{mr}(\lambda_m^{min})}{\lambda_m^{max} - \lambda_m^{min}} (\lambda_m - \lambda_m^{min}) + J_{mr}(\lambda_m^{min}) \quad (185)$$

$$\text{for} \quad \lambda_m^{min} \leq \lambda_m \leq \lambda_m^{max} \quad (186)$$

with $\lambda_m^{min} = -12^o$ and $\lambda_m^{max} = 12^o$. Due to the linear interpolation at each latitude higher frequency modes are introduced which are smoothed by a weighted average in longitude.

$$J_{mr}(j) = \frac{1}{5} [J_{mr}(i+1, j) + 3 J_{mr}(i, j) + J_{mr}(i-1, j)] \quad (187)$$

Since the field–aligned current J_{mr} is used to calculate the ionospheric equator– / downward current sheet contribution $K_{m\lambda}$ the total current system is adjusted automatically to satisfy that it is divergence free.

13.1.2 Eastward current J_{e1} and height integrated current densities $K_{q\phi}$, $K_{q\lambda}$

To calculate the eastward height integrated current density $K_{q\phi}$, see also eq. (7.4) in [Rich95],

$$K_{q\phi} = \int_{h_l}^{h_u} (\frac{R_E + h}{R_0})^{5/2} \frac{J_{e1}}{F} dh \tag{188}$$

the eastward current J_{e1} has to be known. The eastward current J_{e1} is determined by, see also eq. (5.7) in [Rich95],

$$\frac{J_{e1}}{D} = \sigma_P \frac{d_1^2}{D}(E_{d1} + u_{e2}B_{e3}) + (\sigma_P \frac{\mathbf{d}_1 \cdot \mathbf{d}_2}{D} - \sigma_H)(E_{d2} - u_{e1}B_{e3}) + \text{fac}\frac{J_{e1}^{p,g}}{D} \tag{189}$$

The downward–/ equatorward current component J_{e2} is only calculated for postprocessing reasons.

$$\frac{J_{e2}}{D} = \sigma_P \frac{d_2^2}{D}(E_{d2} - u_{e1}B_{e3}) + (\sigma_P \frac{\mathbf{d}_1 \cdot \mathbf{d}_2}{D} + \sigma_H)(E_{d1} - u_{e2}B_{e3}) + \text{fac}\frac{J_{e2}^{p,g}}{D} \tag{190}$$

with fac $= 10^4$ being the conversion factor from $\frac{1}{cm^2}$ to $\frac{1}{m^2}$. The current components are computed on the half pressure levels. The input quantities σ_H, σ_P, $\frac{d_1^2}{D}$, $\frac{\mathbf{d}_1 \cdot \mathbf{d}_2}{D}$, u_{e1}, u_{e2} and B_{e3} are all stored at half pressure levels. Only the electric field E_{d1} and E_{d2} are at full pressure levels and have to be converted to half levels by

$$E_{d1}(k') = \frac{1}{2}(E_{d1}(k) + E_{d1}(k+1)) \tag{191}$$

with k' denoting the half pressure level index $k' = k + \frac{1}{2}$. We assume that $\frac{d_2^2}{D} = 1$ everywhere which is approximately true. In addition to this simplification the height variation of the magnetic field component B_{e3} is neglected. The current contribution due to plasma pressure gradient and gravity $J_{e1}^{p,g}$ is

$$\frac{J_{e1}^{p,g}}{D} = \frac{\mathbf{J}_p \cdot \mathbf{d}_1 + \mathbf{J}_g \cdot \mathbf{d}_1}{D} \tag{192}$$

with $\mathbf{J}_p$ determined in section 9.2 by eq. (123) and the gravity term $\mathbf{J}_g$ in section 9.1 by eq. (118). The gravity and plasma pressure gradient current is calculated in `subroutine magpres_grav` on the geographic grid and is mapped afterward to the geomagnetic grid. Both terms $\mathbf{J}_p$ and $\mathbf{J}_g$ are stored at half pressure levels.

Once the eastward current J_{e1} is determined the height integrated eastward current density $K_{m\phi}$ can be calculated by using eq. (188) with the dipole filed quantity F quantity, see also eq. (6.9) in [Rich95],

$$F = \frac{sin\lambda_m}{sin\lambda_q}\frac{sinI_m}{sinI}(\frac{R_E + h}{R_0})^3 D \tag{193}$$

Inserting eq. (193) into eq. (188) leads to

$$K_{q\phi} = \int_{h_l}^{h_u} \frac{J_{e1}}{D} \frac{sin\lambda_q}{sin\lambda_m} \frac{sinI}{sinI_m} (\frac{R_0}{R_E + h})^{1/2} dh \tag{194}$$

which is calculated at full pressure levels. The height integrated current densities are calculated assuming a dipole field which is indicated by the index $(\cdot)_q$ of $K_{q\phi}$. Therefore the height integration is done in height rather than along the field line. The difference between height and field line integration at mid– and high latitude is small since the field lines are almost vertical through the ionospheric current sheet. The dipole latitude λ_q in eq. (194) is

$$sin\lambda_q(h) = sin\lambda_m(h_0) \tag{195}$$

We assume dipolar field lines such that $\lambda_m(h)$ can be computed by

$$cos^2\lambda_m(h) = \frac{R_0}{R} cos^2\lambda_q \tag{196}$$

The sinus of the inclination angle I_m is determined by

$$sinI_m = \frac{2sin\lambda_m(h_0)}{\sqrt{1 + 3sin^2\lambda_m(h_0)}} \tag{197}$$

and the sinus of the angle I by

$$sinI = \frac{B_z}{|B_0|} \tag{198}$$

with $|B_0|$ the magnitude of the geomagnetic field and B_z the downward component. Note that we assume that both quantities vary in the same way in height and therefore no height variation is taken into account. The equatorial values of $sinI$ and $sin\lambda_q$ are taken from the adjacent grid point in latitude. The height integral is the sum over all height levels with

$$K_{q\phi} = \sum_{k=-2}^{\mathrm{mlev}} S(k') J_{e1}(k') dh(k) \tag{199}$$

with $J_{e1}(k')$ the eastward current at the half pressure level between k and k+1. The term S denotes $\frac{sin\lambda_q}{sin\lambda_m} \frac{sinI}{sinI_m} (\frac{R_0}{R_E+h})^{1/2}$ which is known at the full level e.g. k and k+1 and therefore has to be interpolated to the half pressure level. The discrete height dh is determined by $dh = \frac{1}{100}[z(k+1) - z(k)]$ in [m].
For the calculation of the magnetic perturbations due to plasma pressure gradient and gravity driven current, the height distribution of the eastward current density denoted by $K_{m\phi}^{int}$ has to be known. The previous assumption that most of the current is flowing in a thin current shell is not valid anymore since the current due to gravity and plasma pressure gradient is flowing in the E– and

F–region. Therefore the height dependent current density at pressure level k^* is calculated by

$$K_{m\phi}^{\text{int}}(k^*) = \sum_{k=-2}^{k^*} S(k')J_{e1}(k')dh(k) \tag{200}$$

Once the height integrated eastward current density $K_{q\phi}$ and the radial component of the field aligned current J_{mr} are determined by equations (183) and (199) the height integrated northward current density $K_{q\lambda}$ can be calculated such that the current system is divergence free

$$J_{mr} = \frac{-1}{Rcos\lambda_q}\left[\frac{\partial K_{q\phi}}{\partial \phi_q} + \frac{\partial (K_{q\lambda}cos\lambda_q)}{\partial \lambda_q}\right] \tag{201}$$

Solving eq. (201) for the the height integrated northward current density $K_{q\lambda}$ leads to

$$K_{q\lambda}(\phi_q, \lambda_q^*) = -\frac{1}{cos\lambda_q^*}\int_{-\frac{\Pi}{2}}^{\lambda_q^*}\left[J_{mr}Rcos\lambda_q + \frac{\partial K_{q\phi}}{\partial \phi_q}\right]d\lambda_q \tag{202}$$

The derivative $\frac{\partial K_{q\phi}}{\partial \phi_q}$ is approximated by central differencing

$$\frac{dK_{q\phi}(i,j)}{d\phi_q} = \frac{K_{q\phi}(i+\frac{1}{2},j) - K_{q\phi}(i-\frac{1}{2},j)}{2\Delta\phi_q} \tag{203}$$

with i being the longitudinal index and $i+\frac{1}{2}$ denoting the average between the grid points i and i+1. We substitute the following term for simplicity

$$T(i,j) = J_{mr}(i,j)Rcos\lambda_q(j) + \frac{dK_{q\phi}(i,j)}{d\phi_q} \tag{204}$$

into equation (202). The integration is done over the southern and northern hemisphere separately since the total current in both hemispheres has to cancel.

$$S^{SH}(i,j^*) = -\sum_{j=2}^{j^*} T(i,j-\frac{1}{2})[\lambda_j - \lambda_{j-1}] \quad \frac{nmlat+1}{2} \geq j^* > 2 \tag{205}$$

$$S^{NH}(i,j^*) = \sum_{j=nmlat-1}^{j^*} T(i,j+\frac{1}{2})[\lambda_j - \lambda_{j-1}] \quad \frac{nmlat+1}{2} < j^* \leq \text{nmlat-1} \tag{206}$$

In addition the integral of the absolute northward current is computed by

$$|S^{SH}(i,j^*)| = -\sum_{j=2}^{j^*} |T(i,j-\frac{1}{2})[\lambda_j - \lambda_{j-1}]| \quad \frac{nmlat+1}{2} \geq j > 2 \tag{207}$$

$$|S^{NH}(i,j^*)| = \sum_{j=nmlat-1}^{j^*} |T(i,j+\frac{1}{2})[\lambda_j - \lambda_{j-1}]| \quad \frac{nmlat+1}{2} < j \leq \text{nmlat-1} \tag{208}$$

The northward current $K_{q\lambda}$ has to be corrected to assure that the sum over both hemispheres vanishes. The magnitude of the correction ϵ^{SH} and ϵ^{NH} for the two hemispheres is calculated at each longitude $\phi_q(i)$.

$$\epsilon^{SH}(i) = \frac{1}{2}\frac{S^{SH}(i,j^*) - S^{NH}(i,j^*)}{|S^{SH}(i,j^*)|}| \quad \text{with} \quad j^* = \text{nmlat} \tag{209}$$

$$\epsilon^{NH}(i) = \frac{1}{2}\frac{S^{SH}(i,j^*) - S^{NH}(i,j^*)}{|S^{NH}(i,j^*)|}| \quad \text{with} \quad j^* = \text{nmlat} \tag{210}$$

The corrected northward height integrated current densities in the southern and northern hemisphere are

$$K_{q\lambda}^{cor}(i,j) = \frac{1}{cos\lambda_q}[S^{SH}(i,j) - \epsilon^{SH}(i)|S^{SH}(i,j)|] \quad \frac{nmlat+1}{2} \geq j > 2 \tag{211}$$

$$K_{q\lambda}^{cor}(i,j) = \frac{1}{cos\lambda_q}[S^{NH}(i,j) + \epsilon^{NH}(i)|S^{NH}(i,j)|] \quad \frac{nmlat+1}{2} < j \leq \text{nmlat-1} \tag{212}$$

with the error ϵ distributed according to the weight of $|S(i,j)| = |K_{q\lambda}(i,j)|$. The eastward current J_{e1}, the height integrated current densities $K_{q\phi}$ and $K_{q\lambda}^{cor}$, as well as the height dependent current density $K_{q\phi}^{int}$ are all calculated in `subroutine nosocrdens`.

13.2 No electrodynamo calculation

References

[Peym93] PEYMIRAT, C. AND A. RICHMOND [1993]. 'Modeling the ion loss and the generation of region 2 field–aligned currents via equivalent magnetospheric conductances.' *J. Geop. Res.*, **98**, pp. 15,467–15,476.

[Rich74] RICHMOND, A. [1974]. 'The computation of magnetic effects of field-aligned magnetospheric currents.' *J. Atmos. Terr. Phys.*, **36**, pp. 245–252.

[Rich95] RICHMOND, A. [1995]. 'Ionospheric electrodynamics using apex coordinates.' *J. Geomag. Geoelectr.*, **47**, pp. 191–212.

[Rich05] RICHMOND, A. [2005]. 'Modeling magnetic perturbation from TIEGCM.' *in preparation.*